NIVA

REPORT SNO 4949-2005

Linked models to assess the impacts of climate change on rivers and fjords

Results from a Strategic Institute Programme 2002-2004

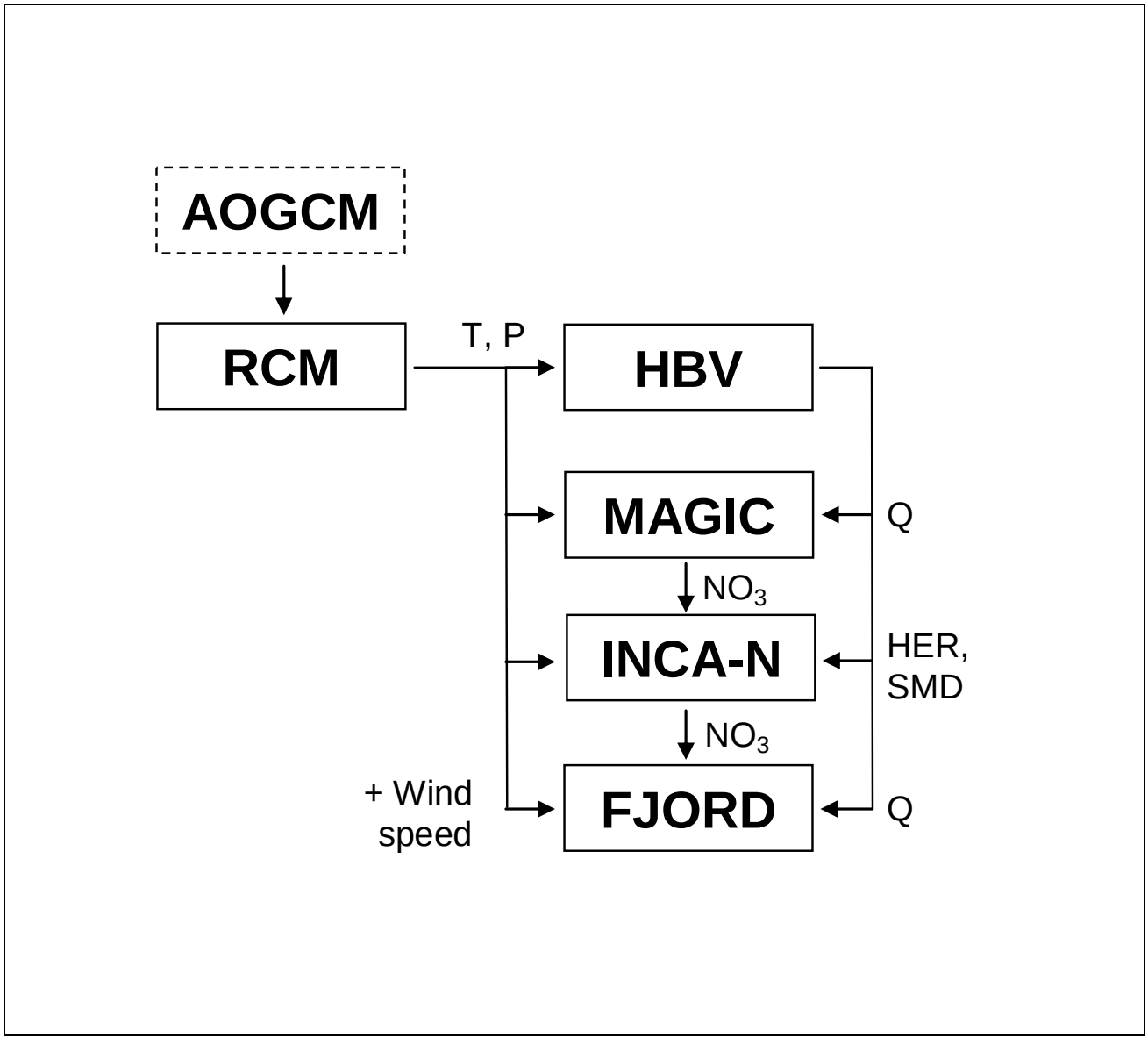

Norwegian Institute for Water Research
– an institute in the Environmental Research Alliance of Norway

REPORT

Main Office
P.O. Box 173, Kjelsås
N-0411 Oslo, Norway
Phone (47) 22 18 51 00
Telefax (47) 22 18 52 00
Internet: www.niva.no

Regional Office, Sørlandet
Televeien 3
N-4879 Grimstad, Norway
Phone (47) 37 29 50 55
Telefax (47) 37 04 45 13

Regional Office, Østlandet
Sandvikaveien 41
N-2312 Ottestad, Norway
Phone (47) 62 57 64 00
Telefax (47) 62 57 66 53

Regional Office, Vestlandet
Nordnesboder 5
N-5008 Bergen, Norway
Phone (47) 55 30 22 50
Telefax (47) 55 30 22 51

Akvaplan-NIVA A/S
N-9005 Tromsø, Norway
Phone (47) 77 68 52 80
Telefax (47) 77 68 05 09

Title	Serial No.	Date
Linked models to assess the impacts of climate change on rivers and fjords. Results from a Strategic Institute Programme 2002-2004.	4949-2005	1. March 2005
	Report No. Sub-No.	Pages Price: 60
Author(s): Øyvind Kaste, Richard F. Wright, Line J. Barkved, Birger Bjerkeng, Torill Engen-Skaugen*, Jan Magnusson and Nils R. Sælthun * *Norwegian Meteorological Institute (met.no)*	Topic group: Climate effects	Distribution: Free
	Geographical area: ROG	Printed: NIVA

Client(s)	Client ref.
The Research Council of Norway, the Commission of European Communities	

Abstract

This report summarises the results from a Strategic Institute Programme (2002-2004), where a linked-model approach has been used to assess the possible impacts of climate change on hydrological, chemical and to some extent biological conditions in a Norwegian river basin and its estuary. Two climate scenarios from two different Atmospheric-Ocean General Circulation Models (AOGCMs) were fed into four individual effect models, linked together and applied at the Bjerkreim river and its estuary, southwestern Norway. The model-chain consisted of the hydrological model HBV, the water chemistry models MAGIC and INCA-N, and the NIVA Fjord Model. The main focus has been on future climate-induced changes in discharge and concentration and flux of nitrogen in the river and its estuary.

4 keywords, Norwegian	4 keywords, English
1. Klimaendringer	1. Climate change
2. Modellering	2. Modelling
3. Overflatevann	3. Surface waters
4. Nitrogen	4. Nitrogen

Øyvind Kaste
Project manager

Brit Lisa Skjelkvåle
Research manager

ISBN 82-577-4643-6

Preface

This work was conducted as part of a Strategic Institute Programme funded in part by the Research Council of Norway 2002-04 and the Eurolimpacs project (the Commission of European Communities GOCE-CT-2003-505540). Additional support came in part from the Norwegian Institute for Water Research. The authors would like to thank Inger Hanssen-Bauer at the Norwegian Meteorological Institute for valuable discussions concerning climate scenarios and Atle Hindar for valuable comments on the manuscript.

Oslo/Grimstad, February 2005

Øyvind Kaste

Contents

Abstract

Dynamically-downscaled data from two Atmosphere-Ocean General Circulation Models (AOGCMs), ECHAM4 from the Max-Planck Institute (MPI), Germany and HADAm3 from the Hadley Centre, UK, driven with two scenarios of greenhouse gas emissions (IS92a and A2, respectively) are used to make climate change prognoses and then to drive four water effect models linked to assess the effects on hydrology and water quality in the 685-km^2 Bjerkreim river basin and its coastal fjord, southwestern Norway. The basic concept was to 1) calibrate and link four existing models to simulate hydrology and water quality (principally nitrogen concentrations) at present climate, and then 2) simulate possible effects of two different climate change scenarios. The four effect models were the hydrological model HBV, the water quality models MAGIC and INCA-N, and the NIVA Fjord Model. The two downscaled climate scenarios project a general temperature increase in the study region, ~1^{o}C with MPI IS92a (2030-2049) and ~3^{o}C with Hadley A2 (2071-2100), and also increased winter precipitation. Projections of summer and autumn precipitation are quite different, however, with the MPI scenario projecting a slight increase whereas the Hadley scenario implies a significant decrease. As a response to the scenarios the HBV model simulates a dramatic reduction of snow accumulation in the upper parts of the catchment, which in turn lead to higher runoff during winter and reduction of the snowmelt flood. With the Hadley scenario runoff in summer and early autumn is substantially reduced, as a result of reduced precipitation, increased temperatures and thereby increased evapotranspiration. The water quality models MAGIC and INCA project no major changes in N concentrations and fluxes with the MPI scenario, but a significant increase in NO_3 concentrations and a 40-50% increase in N fluxes with the Hadley scenario. As a consequence the acidification of the river could increase, thus offsetting ongoing recovery from acidification due to reductions in acid deposition. Additionally, the increased N loading may govern growth of N-limited benthic algae and macrophytes along the river channels and lead to undesirable eutrophication effects in the estuarine area. Simulations made by the Fjord model indicate that summer production in the estuary might increase by at least 15-20 % with the Hadley scenario. At present, there is a large scatter in the proposed climate scenarios, and additionally the climate system often is represented differently in the various AOGCMs. This uncertainty will in turn be propagated through effect-chain via hydrology, to water chemistry and biology. An important task for the future will therefore be to quantify this uncertainty, both related to the climate scenarios and the effect models applied.

1. Introduction

Current scenarios developed for future climate in northern Europe project long-term increases in air temperature, and some of them also more rainfall and increased frequency and severity of extreme rainfall and storms (Cubasch *et al.* 2001; Førland *et al.* 2000; Palmer and Räisänen 2002). The rate of change will vary by region, with significant east-west and south-north gradients in both temperature and precipitation. Additionally, different Atmospheric-Ocean General Circulation Models (AOGCMs) include differences in the projected change of large-scale circulation patterns that may have a large influence on the regional distribution of rainfall (Benestad 2002). Hence, there is currently a relative large variation in the predictions for future climate change in this region.

There is a close connection between the climate system and hydrological, chemical, and biological processes in catchments. Even small changes in ambient climate may induce a series of inter-related responses in terrestrial and aquatic ecosystems. For example, at intermediate altitudes in southern Norway a temperature increase during winter may cause significant reductions in snow accumulation, which in turn might give more frequent freezing-thawing events, more winter floods, strongly diminished spring melt flood and a prolonged growing season. On the other hand, increased winter precipitation in the future may cause an increase in snow accumulation at higher altitudes (Raold *et al.* 2002).

Soil temperature and soil moisture are important regulators of biogeochemical processes in catchments. An increase in soil temperature will speed up the decomposition of organic matter and thereby increase the availability of inorganic nutrients by mineralisation. The result may be increased leaching of dissolved organic compounds and inorganic nitrogen species, especially nitrate (NO_3^-). Monitoring data from several streams and lakes in northwestern Europe and eastern USA show increasing trends in dissolved organic carbon (DOC) over the last 10-15 years (Freeman *et al.* 2001; Skjelkvåle *et al.* 2001; Stoddard *et al.* 1999). Several authors have suggested a close connection between the observed trends and a change in ambient climate. The effect of increased temperature on leaching of N and C was demonstrated experimentally on a whole-catchment scale in the CLIMEX project that was performed at Risdalsheia in southernmost Norway (Van Breemen *et al.* 1998; Wright 1998). Here, a 3.7^{o}C increase in annual air temperature over three years accelerated the decomposition of soil organic matter and induced a three-fold increase in the leaching of inorganic N.

Long-term and episodic changes in hydrological regime and element fluxes might have important implications for water quality and biology in streams and lakes. In fjords and coastal waters, eutrophication status and deep-water renewal can be affected by climate change – either directly through large-scale changes in air temperature, solar radiation, wind speed, wind direction, or indirectly by changes in the coastal current or riverine inputs of freshwater and nutrients.

To assess the possible impacts of climate change on hydrological, chemical and to some extent biological conditions in a Norwegian river basin and its estuary we have fed two climate scenarios from two different AOGCMs into four individual effect models. The models are linked together and applied at the Bjerkreim river and its estuary, southwestern Norway. The model-chain consists of the hydrological model HBV, the water chemistry models MAGIC and INCA-N, and the NIVA Fjord Model. The focus is on future climate-induced changes in discharge and concentration and flux of nitrogen in the river and its estuary.

2. Materials and methods

2.1 Site description

The Bjerkreim river

The Bjerkreim river has an average runoff of 2430 mm yr^{-1} and discharges into an estuarine area (58°28'N; 5°59'E) near Egersund in southwestern Norway (Figure 1). The 685 km^2 basin consists of three main tributaries from northeast, and one minor tributary from northwest. There are several relatively large lakes, especially in the eastern part. Bedrock geology is Precambrian granitic gneisses, anorthosite and leuconorite. The land cover of the Bjerkreim basin, dominated by non-forested, mountainous areas (~60 %), is typical of the inner southwestern parts of Norway. Water surfaces, peatlands and heathlands make up about 20 % of the land area, while forests and agricultural land cover 15 % and 5 % each (Table 1). About one quarter of the forest stands are coniferous, the rest are deciduous.

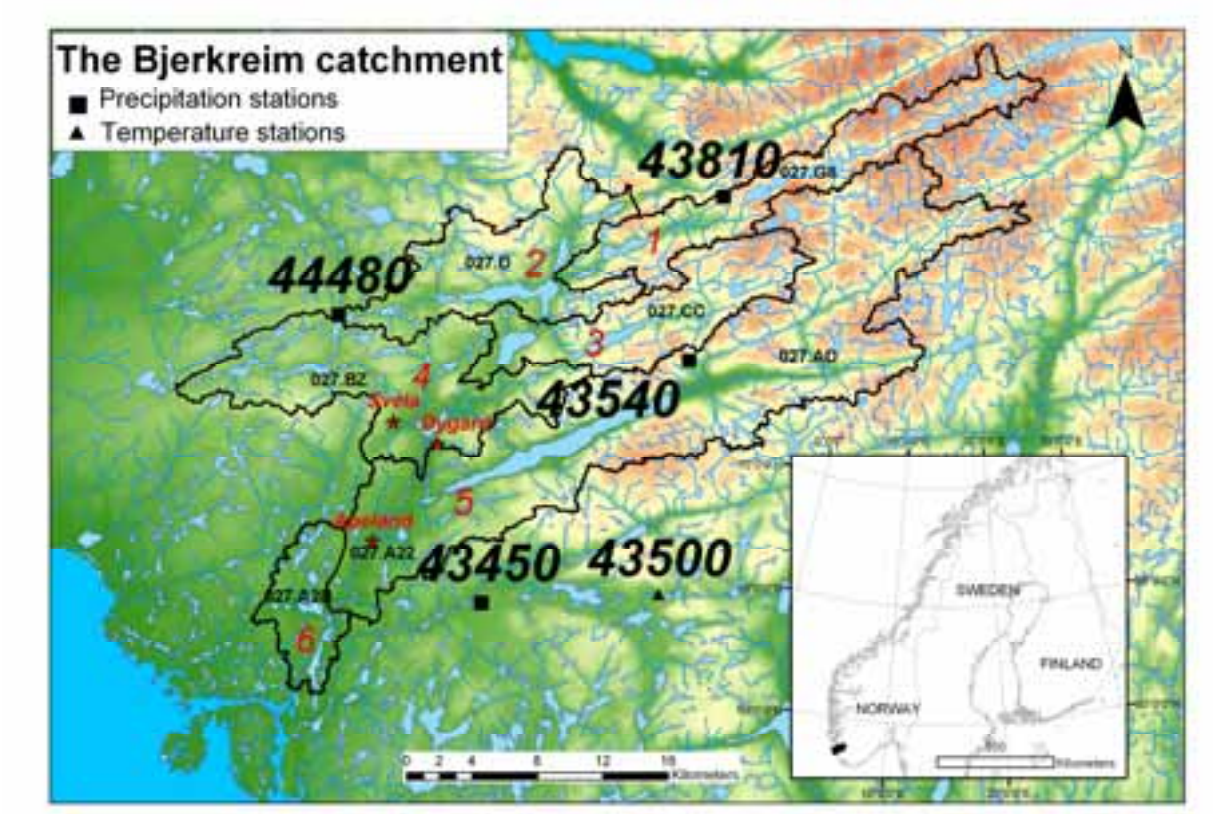

Figure 1. Map showing the Bjerkreim river basin with precipitation stations (squares) and temperature station (triangle) (with Norwegian Meteorological Institute station codes), sub-basins 1-6 (with NVE-REGINE codes) and locations of the three small catchments Øygard, Svela and Apeland (stars).

The Norwegian project "Nitrogen from mountains to fjords" conducted in 1992-96 studied the nitrogen input, internal cycling and output in catchments and lakes in the Bjerkreim river basin (Henriksen and Hessen 1997). Several small catchments with contrasting dominant vegetation and land-use were studied (Kaste *et al.* 1997). Data from two of these, Øygard (2.55 km^2, typical semi-natural upland terrain with heather and mountain birch vegetation) and Svela (0.51 km^2, predominantly Norway spruce plantation from the 1920s), were used in the modelling work here.

N deposition in the Bjerkreim area is the highest in Norway, 15-23 kg N ha^{-1} yr^{-1} (wet + dry) due to both high precipitation rates and relatively high N concentrations (Tørseth and Semb 1997). Average rates of precipitation vary from 1.5 m yr^{-1} in the lower southwestern parts to about 3.5 m yr^{-1} at higher

altitudes in the northeastern part (Tørseth and Semb 1997). The basin is sparsely populated (only 3.5 inhabitants km^{-2}), and atmospheric deposition is the dominant N source in the basin as a whole. Settlement and agriculture are mainly concentrated at lower elevations, where local N inputs can contribute significantly to the total N load.

Table 1. Land cover distribution in the Bjerkreim river basin, including sub-basins and small catchments. Data from the Norwegian Institute of Land Inventory (NIJOS).

	Size	Land cover distribution (%)					
	km^2	Forest	Heath	Peat	Pasture	Arable	Lakes
Bjerkreim river basin	685	18	64	1	4	2	11
Sub-basin 1	87	11	74	1	1	1	12
Sub-basin 2	67	27	44	1	6	4	18
Sub-basin 3	79	17	66	1	2	1	13
Sub-basin 4	117	22	51	2	12	5	8
Sub-basin 5a	259	12	75	1	1	1	11
Sub-basin 5b	40	38	31	1	15	10	5
Sub-basin 6	36	35	43	1	5	3	13
Svela catchment	0.6	61	39	-	-	-	-
Øygard catchment	2.5	4	83	6	-	-	7
Apeland catchment	1.7	60	9	-	23	10	-

The Egersund Estuary.

The Egersund Estuary has two connections to the North Sea (Figure 2). The northern part (Nordre Sundet) is separated from the southern by a narrow sill, 2 m deep and 30-60 m wide. The river Bjerkreim discharges to Tengsvågen and mixes with seawater, mainly in the northern branch of the estuary. In the model setup here the northern branch is chosen as the model area and the connection to the southern branch is closed. The northern branch (Nordre Sundet) consists of a series of small shallow basins, separated by sills (2-5.5 m deep) or narrows (60 – 500 m wide). The surface area is about 3.8 km^2 and the main sill depth 5.5 m. The deepest point inside the main sill is 18 m, but on the whole the deeper part varies between 8-12 m depth. The estuary has a typical estuarine circulation, with outflowing brackish water and inflowing sea-water.

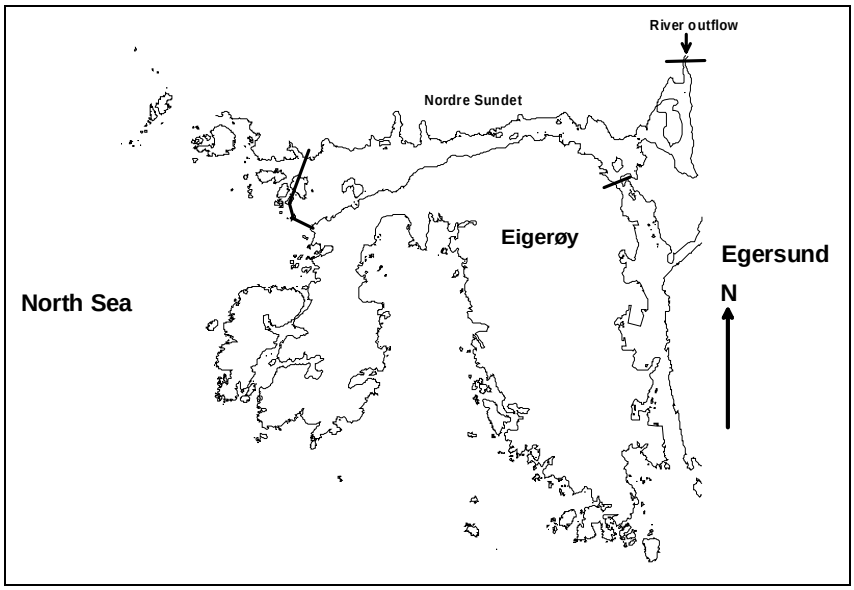

Figure 2. The Egersund Estuary, with two branches: the northern branch in an east-west direction (called Nordre Sundet) and the southern branch in a north-south direction). Limits of model area are shown with thick lines.

2.2 The models

The downscaled AOGCMs and the four effect models HBV, MAGIC, INCA-N and FJORD were linked together in the sense that each model produced input data to the next. The models were not physically linked, and there were no feedback mechanisms or process integration between the models. The four effect models were first calibrated on the basis of observed data (Figure 3). Then they were run with future climate parameters from the two AOGCMs (cf. Table 2). HBV used dynamically downscaled climate data together with basin characteristics to produce runoff on daily time steps. These hydrologic data and the climatic data were fed into the MAGIC model together with data for atmospheric N deposition and soil chemistry to simulate N concentrations (and other major ions) in runoff at annual time steps. The hydrologic data from HBV, the runoff N data from MAGIC, and the climatic data were fed into INCA-N, an integrated N and water routing model for river basins, together with deposition and point source data to simulate daily discharge and concentrations of inorganic N in the river. Finally, the NIVA Fjord model used the time series data from INCA-N for the different climate scenarios, meteorological data¸ morphological data for the fjord and information on the mixing with the coastal current to simulate effects of changed climate forcing, hydrology and N inputs on physical, chemical and biological conditions in the estuarine area.

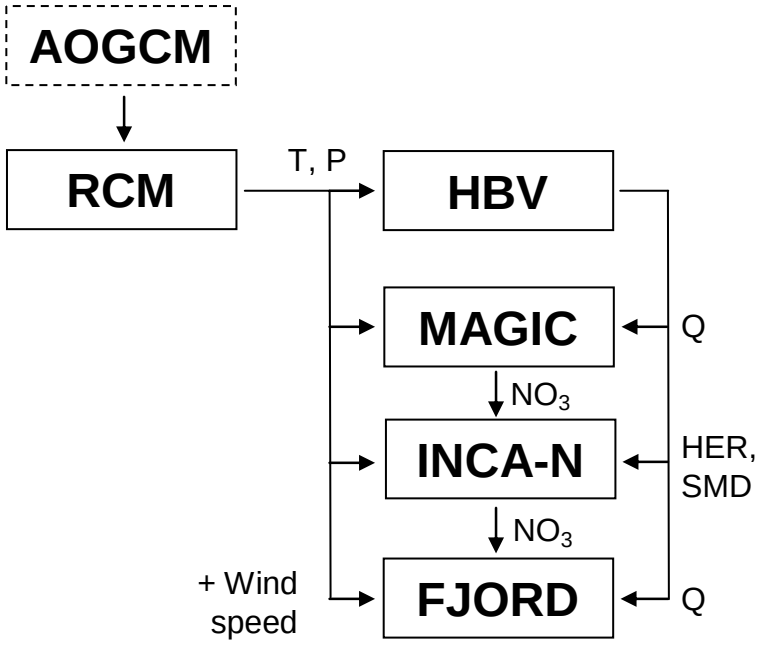

Figure 3. The linked-model approach. Data transfer between the models is indicated by arrows. T = air temperature, P = precipitation, Q = water flow, HER = hydrologically effective rainfall, SMD = soil moisture deficit.

Climate models and downscaling
Two different AOGCMs are used in the study; the ECHAM4/OPYC3 model developed at the Max Planck Institute (MPI) in Germany with the GSDIO integration (Roeckner *et al.* 1999) and HadAm3 model developed at the Hadley Centre, UK (Gordon *et al.* 2000). The spatial resolution of AOGCMs is typically ~300 x 300 km^2. Thus, to obtain reliable estimates of the climate at specific regions in Norway, downscaling is necessary. Results from AOGCMs are dynamically downscaled with the regional climate model HIRHAM (Bjørge *et al.* 2000). HIRHAM is similar to the model used at MPI and the Danish Meteorological Institute (DMI) and is based on the dynamics of the weather forecast model HIRLAM which is operationally used at the Norwegian Meteorological Institute (met.no) and the physics of ECHAM4. HIRHAM has a spatial resolution of ~55 x 55 km^2. The resulting physical parameters have a 6-hour time resolution and there is consistency between the parameters.

HIRHAM is run with one control period and one scenario period. The control run represent the model's realisation of the present climate. The estimated day-to-day variability is thus not comparable

with observations, but the mean monthly values and standard deviation based on daily values should be comparable. The models are run with two different emission scenarios, IS92a and A2 (Cubasch *et al.* 2001). Up to 2050 IS92a gives slightly lower increase in global temperature than A2. Up to 2100 IS92a gives approximately 2.3 °C increase in global temperature while A2 is giving an increase of approximately 3.4 °C. ECHAM4/OPYC3 is run with emission scenario IS92a (called the MPI scenario), and HadAm3 is run with emission scenario A2 (called the Hadley scenario). The two model runs have different control periods and scenario periods (Table 2).

Table 2. The Atmospheric-Ocean General Circulation Models (AOGCMs) and emission scenarios used with control period and scenario period.

Model	Emission scenario	Control period	Scenario period
ECHAM4/OPYC3	IS92a	1980-1999	2030-2049
HadAm3	A2	1961-1990	2071-2100

Daily measurements of temperature and precipitation at individual stations are traditionally used as input to the hydrological model chain. Estimates of temperature and precipitation are therefore interpolated from HIRHAM to selected locations. There are often difficulties associated with this, e.g. the station altitude is often incorrectly represented in the model and the number of rainy days is typically overestimated (Frei *et al.* 2003). The dynamically-downscaled temperature and precipitation data are therefore empirically adjusted to be representative on a local scale. The adjustment procedure is described in (Engen-Skaugen 2004). The twenty years 1980-1999 was used as control period, in order to match available time series of observed water flow and chemistry in the Bjerkreim river basin (1980 – to date). The dynamically-downscaled HadAm3 data for the control period 1961-1990 were adjusted with the same procedure, but the statistics were tuned to be representative for the period 1971-2000, rather than the original control period 1961-1990. To make the scenarios even more comparable, only the twenty last years in the Hadley run were used (Table 2).

HBV

The HBV model is by far the most applied operational hydrological model in Scandinavia. It was originally developed in the 1970s at the Swedish Meteorological and Hydrological Institute (Bergström 1976). Several versions of the model exist and in this study a version of the model developed for the project Climate Change and Energy Production (Sælthun 1996; Sælthun *et al.* 1998) has been applied. The HBV model can be classified as a semi-distributed conceptual model with subdivision in altitude zones and distributed snow and soil moisture description. The HBV model is regarded adequate for use in this study, where the multi-model approach is in focus rather than a detailed study of the hydrological processes. The general model structure consists of four main components: a snow module, a soil moisture zone module, a dynamic module comprising the upper and lower soil zone, and a routing module (Figure 4). Model simulations are run on a daily time step. The HBV model parameters can be grouped into two main categories, free and confined parameters (Killingtveit and Sælthun 1995).The confined parameters are based on physical measurements and not subject to calibration, for instance catchment area, area elevation curve and lake percentage. The free parameters must be determined by calibration.

The model was set up for three small catchments, Øygard, Svela and Apeland, and seven medium-sized sub-basins within the Bjerkreim basin (sub-basin 5 is divided in two units; Figure 1). HBV contributes to the other models with simulated daily runoff values (Q) based on downscaled climate change scenarios of P and T series. Further, the model gives calculated temperature series corresponding to the average height in the catchments and calculated area precipitation for the catchments. The areal precipitation is based on point correction for rainfall and snowfall measurement errors, fixed station weights and linear altitude increase of precipitation. These data are used by the MAGIC model. It also provides estimates in mm/d of hydrological effective rainfall (HER: the part of

the precipitation/snowmelt that contributes directly to runoff) and soil moisture deficit (SMD) to the INCA-N model. In the HBV model the HER is calculated by the following steps:

- Input to the soil moisture zone is precipitation minus interception on vegetation in snow free areas.
- In snow covered areas the input to the soil moisture zone is yield from the snow pack, calculated as snow melt plus rain, but attenuated through the liquid water holding capacity of the spatially distributed snow pack.
- In the soil moisture zone, the input is split in two parts, HER and contribution to the soil moisture content. The splitting factor is dependent on the soil moisture content (catchment wetness).

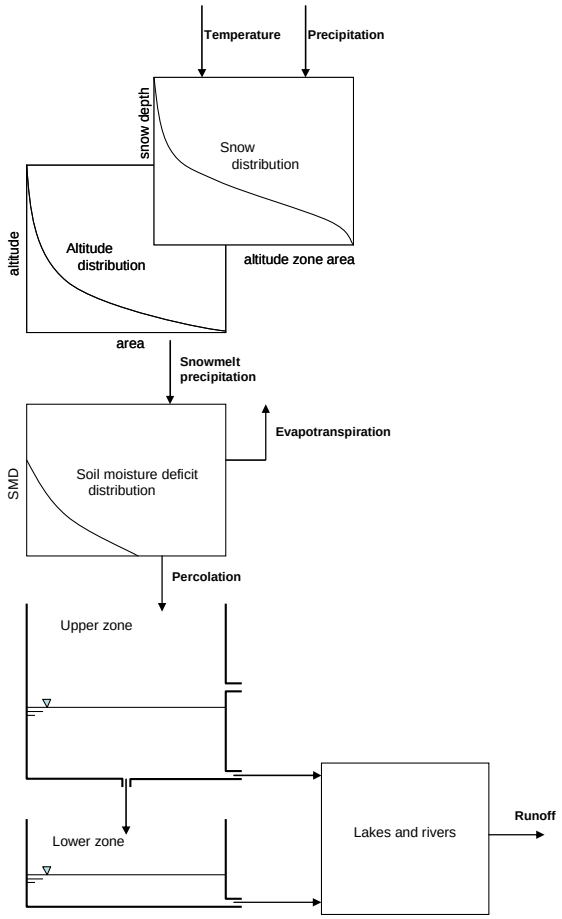

Figure 4. A schematic depiction of the HBV model. After Sælthun (1996).

The soil moisture content is calculated as the accumulated balance between the input, described above, and the actual evapotranspiration. The actual evapotranspiration is a function of the soil moisture content and the potential evapotranspiration, being equal to potential evapotranspiration at field capacity. Soil moisture deficit is the difference between field capacity and soil moisture content. Potential evapotranspiration is calculated by a simple temperature index model. There are indications that this model may overestimate the effect of temperature rise on potential evapotranspiration (Sælthun *et al* 1998).

MAGIC

MAGIC is a lumped-parameter model of intermediate complexity, developed to simulate the long-term effects of acidic deposition on surface water chemistry (Cosby *et al.* 2001; Cosby *et al.* 1985a;b). The model simulates soil solution and surface water chemistry to simulate the average concentrations of the major ions. In the applications here, MAGIC was used only to simulate the long-term annual-

mean concentrations and fluxes of inorganic N compounds in streamwater. Major N processes incorporated explicitly or implicitly into the model are atmospheric deposition, nitrification, denitrification, mineralisation, uptake by plants, litterfall, decomposition, immobilisation into soil organic matter, and export in runoff (Figure 5). N fixation is assumed negligible. The soil organic matter pool is aggregated in space to encompass the whole basin and in time to annual timesteps. The N and C contents of the organic matter pool are state variables simulated by the model in response to changing inputs or outputs. MAGIC also includes a description of N retention in lakes. This is based on the empirical model of Dillon and Molot (1990) as tested for Norwegian lakes by Kaste and Dillon (2003) in which N retention is related to the hydrologic flushing time and NO_3 and NH_4 concentrations in lakewater.

The N dynamics in soil are based conceptually on the empirical model described by (Gundersen *et al.* 1998) in which N retention is assumed governed by the C/N ratio of the soil organic matter. If the soil organic matter has a high C/N ratio (i.e. N-poor), all NH_4 and NO_3 in soil solution is immobilised, whereas if the C/N ratio is low, no N is immobilised. This is described in MAGIC by a simple function requiring specification of only two parameters, the upper C/N ratio at which immobilisation is 100% and the lower C/N ratio at which immobilisation is 0% (Figure 6). This model assumes that the inorganic N immobilised from soil solution is added to the soil organic matter pool, lowering its C/N ratio. Chronic N deposition and N immobilisation will thus lead to a decline in the C/N ratio of the soil organic matter pool. When the C/N crosses the upper threshold, leaching of inorganic N begins and gradually increases as C/N declines further.

Data inputs required for calibration of N dynamics in MAGIC comprise lake and catchment physical characteristics, soil C and N pools and physical characteristics, input and output fluxes for water and inorganic N compounds, and estimates of denitrification, nitrification, net uptake of N by vegetation and litterfall of N. In calibration the upper C/N ratio is fitted to match observed NO_3 and NH_4 concentrations in streamwater, and the slope of the line in Figure 6 is specified. Changes over time of the size of the soil C pool must also be specified.

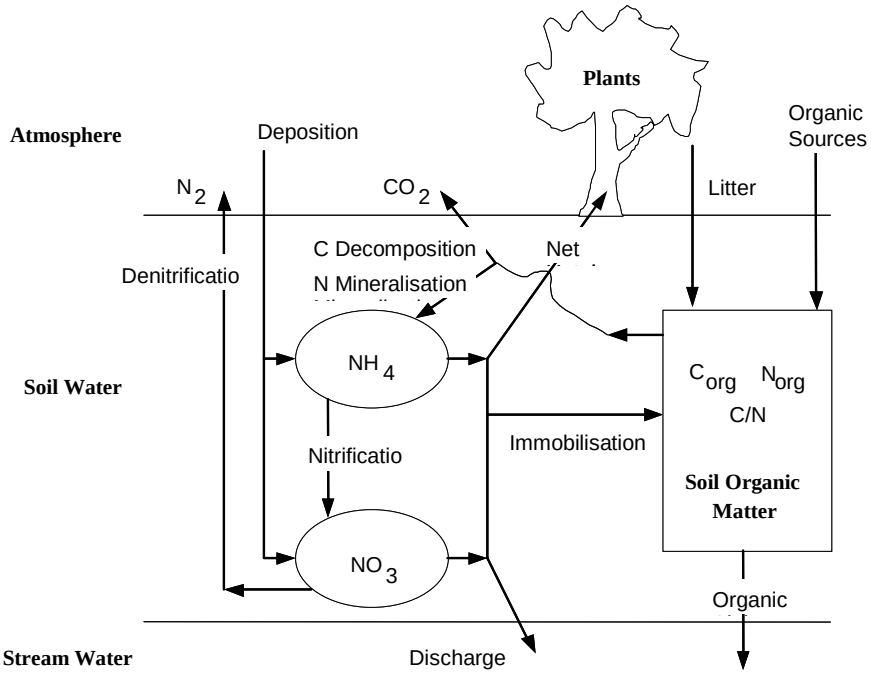

Figure 5. Schematic depiction of the pools and fluxes included in MAGIC (version 7) used to simulate the dynamics of organic and inorganic N in soils and streamwater. From Cosby *et al.* (2001).

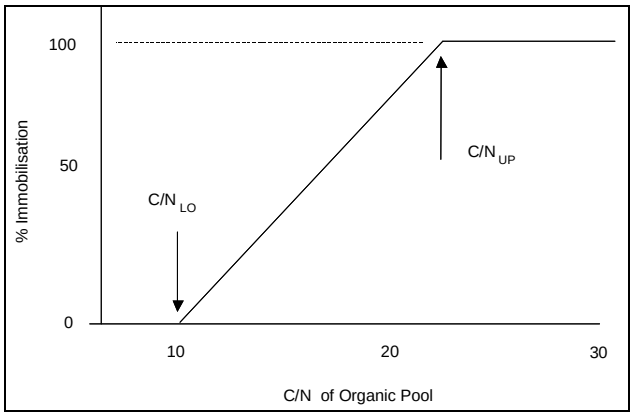

Figure 6. Schematic depiction of N retention in soil based on the empirical model of (Gundersen *et al.* 1998) and used by MAGIC.

INCA-N

The process-based and semi-distributed Integrated Nitrogen in Catchments model (INCA-N) developed by (Whitehead *et al.* 1998) has recently been revised (version 1.6) and described in detail by (Wade *et al.* 2002). The model integrates hydrology, basin and river N processes, and simulates daily NO_3 and NH_4 concentrations as time series at key sites, as profiles down the river system, or as statistical distributions. The term semi-distributed is used, as it is not intended to model the catchment land surface in a detailed manner. River, soil water and ground water NO_3 and NH_4 concentrations and fluxes are produced as daily time series.

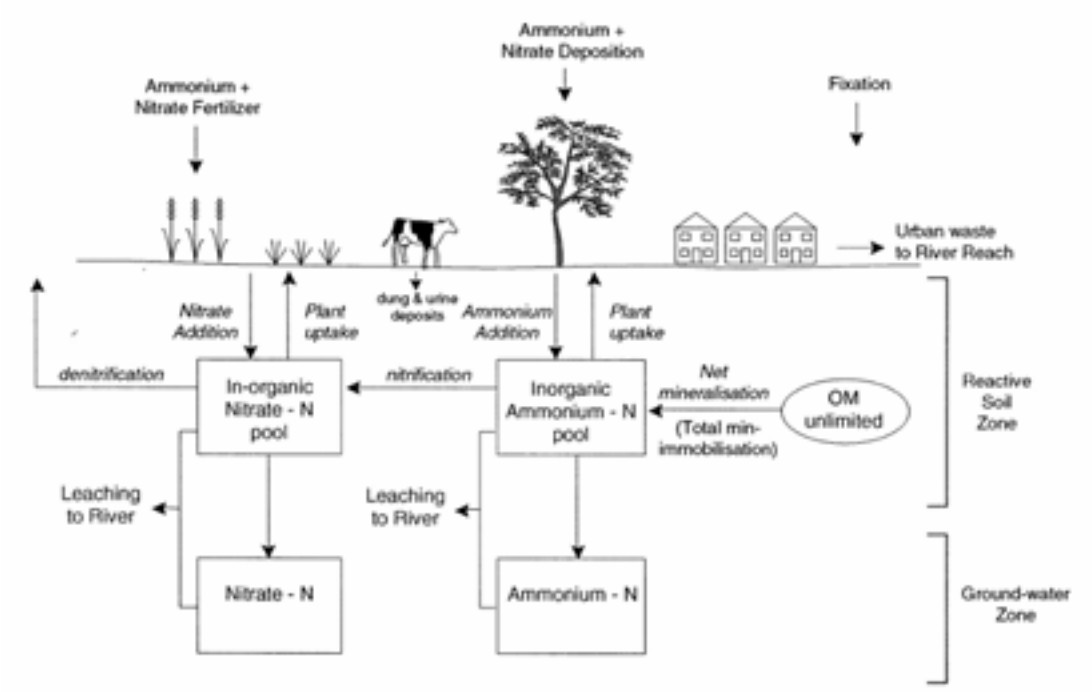

Figure 7. N plant/soil system processes included in the INCA-N model. After Whitehead *et al.* (1998).

Three components are included: the hydrological model, the catchment N process model (Figure 7), and the river N process model (Figure 8). Sources of N include atmospheric deposition, the terrestrial environment and direct discharges. Hydrological processes in soil are simulated in the hydrological sub-model. This requires input of daily time series of T, P, SMD, and HER. The mass balance equations for NO_3 and NH_4 in both the soil and groundwater zones are solved simultaneously with the

flow equations. The key N processes modelled in the soil water zone are nitrification, denitrification, mineralization, immobilisation, N fixation and plant uptake of mineral N. Rate coefficients of N processes are temperature and moisture dependent.

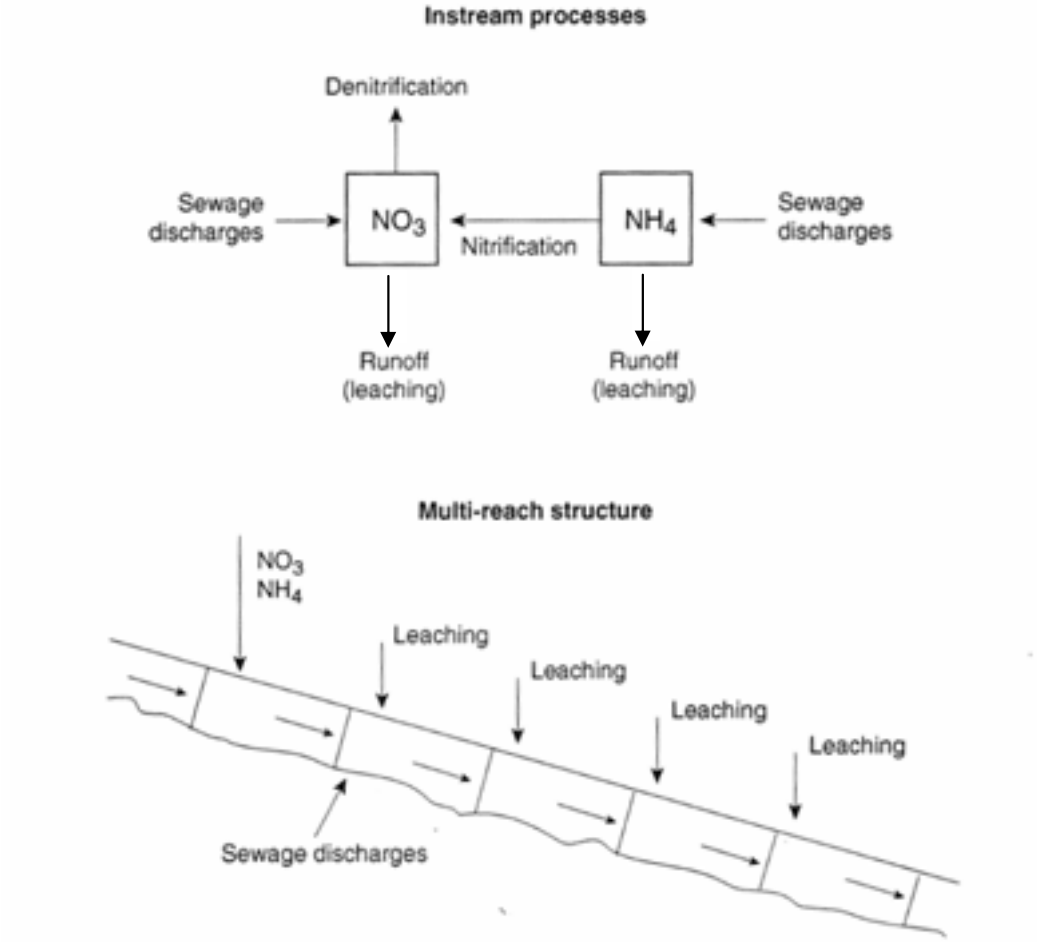

Figure 8. Riverine N processes and transformations included in the INCA-N model. After Whitehead *et al.* (1998).

To improve the simulation of N transformation rates in northern catchments, characterised by cold climates and extensive snow accumulation during winter, a slightly modified version of the model (v. 1.7) was developed by (Rankinen *et al.* 2004). This was achieved by inclusion of a simple, empirical function to simulate soil temperatures below the seasonal snow pack, a degree-day model to calculate the depth of the snow pack, and a modified temperature response function for N processes based on Q_{10} values (Figure 9). In the most recent version of the model (v. 1.9), it is possible to apply individual temperature response functions for each process and each land cover class. These modifications have substantially increased its flexibility and applicability for climate effect studies. Thus INCA-N v. 1.9 was applied in this study.

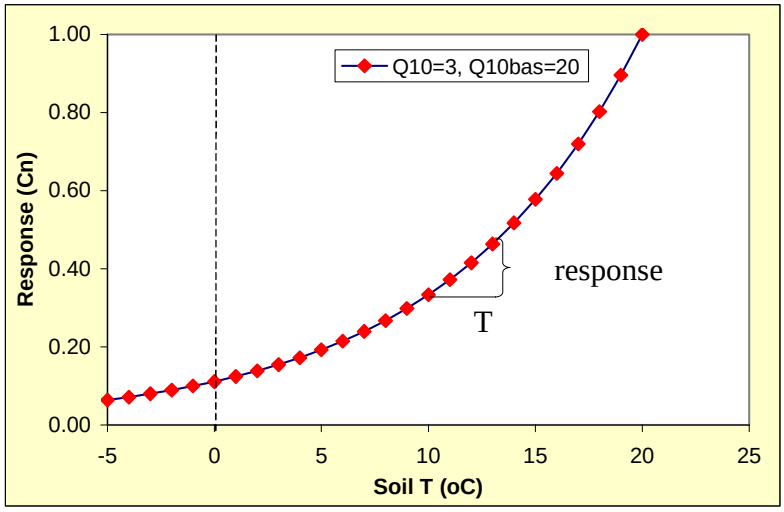

Figure 9. Example temperature response function for N processes included in the INCA-N model. The parameter Q_{10} is the factor change in rate with a 10 degree change in temperature, and the parameter Q_{10bas} is the base temperature for the N process at which the response is 1.

NIVA Fjord model
The NIVA fjord model describes eutrophication response to nutrient and organic matter loading through simulation of primary production, sinking and degradation of organic matter (Bjerkeng 1994). The chemical/biological processes are described in a physical framework with the fjord divided in a variable number of basins, each basin divided vertically in a variable number of layers. Vertical mixing within each basin and horizontal transports between basins are dynamically coupled to the density field within each basin and to the difference in density fields of interconnected basins. Empirical relations between mixing and vertical stratification are used to describe vertical mixing.

The biological submodel for the water column and benthos describes primary production by phytoplankton, divided in two groups with different characteristics (loosely characterized as diatoms and flagellates), grazing by zooplankton and mussels. Primary production is considered to be a function of light, temperature, available nitrogen and phosphorus and for diatoms also silicate. Diurnal variations are included. The model also includes excretion of DOC and bacterial growth connected to DOC. Particle sinking and degradation in water and sediment under different oxygen regimes including denitrification are described by dynamic sub-models. The model is driven by data for discharge from the river, weather (T, P, and wind speed) and conditions on the outer boundary as functions of time.

2.3 Input data

Climate and hydrology
Daily values of T and P are the driving variables of the HBV model and daily discharge measurements are needed for calibration of the model. HBV uses weighted station measurements of T and P to represent the river basin area. The HBV model was calibrated to each of the selected sub-basins using five P stations and one T station operated by the Norwegian Meteorological Institute (met.no) (Figure 1; Table 3; Figure 10). Daily temperature values after March 1997 at station 43500 Ualand were estimated by spatial interpolation based on neighbouring stations. The method is described in (Tveito *et al.* 2000). Daily discharge measurements are available for the small catchments Øygard 1993-1999, Svela 1993-1995, Apeland 1993-1995 (gauging stations operated by NIVA), and in the main river at Gjedlakleiv (catchment: 618 km^2; gauging station operated by the Norwegian Water Resources and Energy Directorate - NVE).

The NIVA Fjord model was run with 6-hour historical observations (1981-1995) of T, P and wind speed from the coastal weather station Lista Fyr (58°07'N; 6°33'E; about 52 km SE of the Egersund estuary).

Table 3. Station name and station number, observation period and parameter used (precipitation, P, or a temperature, T) at the selected stations. Station altitude (H_1) and corresponding altitude in the HIRHAM regional climate model (H_2) is presented in the table.

Station	Observation period	Data type	H_1 (m)	H_2 (m)
43450 Helleland	1895-to date	P	94	215
43540 Ørsdalen	1923-to date	P	70	330
44480 Søyland	1902-to date	P	263	216
43810 Maudal	1946-to date	P	311	376
43500 Ualand	1968-1997	T	196	271

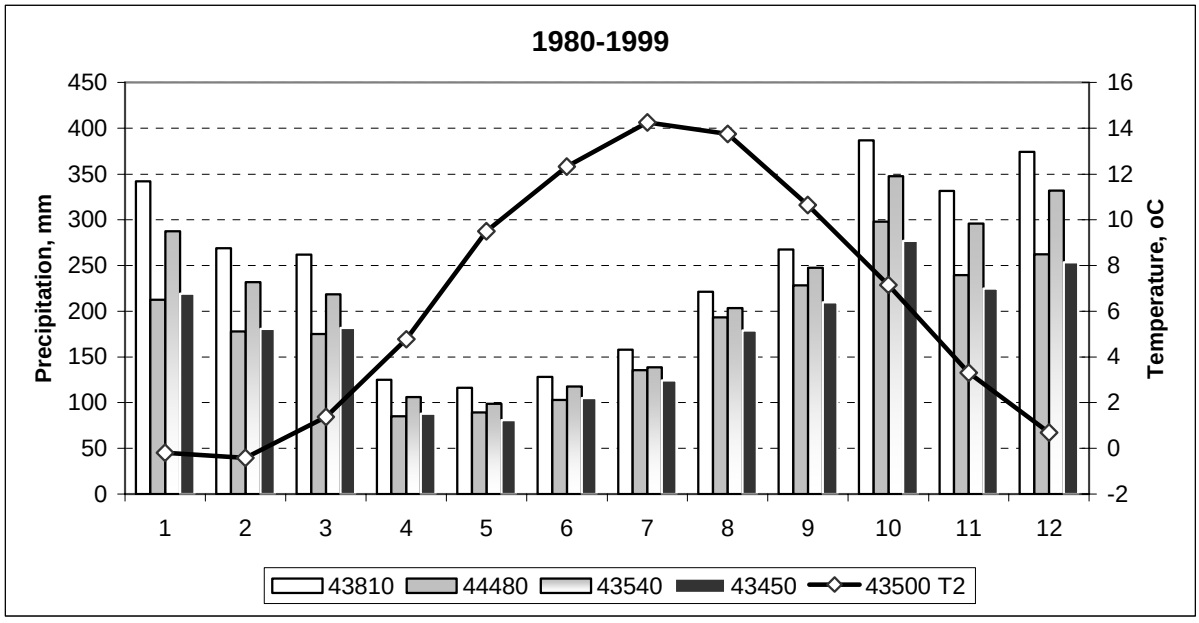

Figure 10. The control period, 1980-1999: Mean monthly precipitation and temperature at selected stations

Freshwater chemistry

Chemical data for nitrogen components for the Bjerkreim river come from monthly samples collected at the outlet from 1980 to date, within the framework of the Norwegian monitoring programme on long-range transported air pollutants (LRTAP) (SFT 2004). During 1993-1995 fortnightly samples were collected from 20 additional surface water sites within the Bjerkreim river basin as part of the research project "Nitrogen from mountains to fjords" (Henriksen and Hessen 1997). Among these were the small catchments Øygard (heath), Svela (forest) and Apeland (agriculture). Since 1996, the monitoring at Øygard has continued as part of the Norwegian LRTAP programme. All samples have been analysed unfiltered at NIVA for major components including nitrate (NO_3) and ammonium (NH_4). Whereas NO_3 data are available from the whole sampling period, only single years with NH_4 data exist (1988 and after 1999).

The NIVA Fjord model also requires information for runoff concentrations of orthophosphate, silicate, oxygen and organic particulate carbon, nitrogen and phosphorus, as well as dissolved organic carbon. Orthophosphate has not been measured regularly in the Bjerkreim river, but there are data on total phosphorus, with values varying between 2.9 and 11 $\mu g\, L^{-1}$. This is about the same concentration level

as in River Otra, which is part of the national river monitoring programme. Here, the concentrations of orthophosphate are generally low and mostly in the range 0.5 – 1.0 µg $P L^{-1}$ (max 12 µg $P L^{-1}$). Orthophosphate in River Otra is not clearly related to either water flow, season, total phosphorus or nitrate, but has a log-normal distribution, $\log_{10}(PO_4P[\mu g P L^{-1}])$, with average -0.019 and standard deviation 0.30. Orthophosphate concentrations for the Bjerkreim runoff scenarios are based on random draws from this statistical model, using the same series in all scenarios.

Silicate data from the Bjerkreim river are available for the years 1992 to 1996. About 59 % of the silicate variance in these data can be accounted for by a non-linear model on season and water flow *q*:

$$[SiO_2(mg/l)] = \frac{\{2.105 + 0.2863 \cdot (\sin(2\pi(t + 0.2511)))\}}{q^{0.1}}$$

where *q* is water flow (m^3/s) and t is time from January 1 in unit *year*. The residuals, with standard deviation about 1.5 mg L^{-1}, show no sign of autocorrelation between succeeding observation dates which are mainly 14 days apart. For the simulations, this model has been applied individually to each date of the INCA-N output series, with differences in water flow being reflected in the silicate values. The fit could have been improved by including nitrate as covariate, but since we cannot assume that the relation between silicate and nitrate would be the same under a climate change, this has not been done.

Particulate organic matter in the runoff from the Bjerkreim river is ignored in the simulations, with concentrations of particulate as C, N and P in the runoff being set to zero in all scenarios. Dissolved organic carbon is modelled using data for total organic carbon. The data show no clear relation to either season or water flow, but approximately log-normally distributed concentrations with $\log_{10}(TOC\ mgC\ L^{-1})$ having average 1.0 and st. deviation 0.1.

The runoff temperature is taken from meteorological observations for the period 1980-2000, exponentially smoothed over 4 days and with a lower limit of 0 °C, and oxygen concentrations are calculated by assuming saturation as function of temperature. The oxygen content and temperature of the runoff was not changed between scenarios.

External N sources in the Bjerkreim river basin

The major external N source in the Bjerkreim river basin is atmospheric deposition, whereas direct inputs of sewage and agricultural effluents are small and mainly restricted to the lower parts of the catchment (Kaste *et al.* 1997). The atmospheric N deposition data applied in this study are derived from the monitoring stations Ualand and Skreådalen (Figure 1), both included in the LRTAP programme (Aas *et al.* 2004). The data comprise wet and dry deposition of total inorganic N (TIN; the sum of NO_3^- and NH_4^+) Wet deposition is determined by the chemical composition and amount of precipitation, whereas dry deposition is estimated from ambient air concentrations and dry deposition velocities for individual components (Tørseth and Semb 1998). For the period 1993-95 (Tørseth and Semb 1997) estimated a precipitation amount- and N deposition field for the Bjerkreim river basin. The fields were based on runoff data from 44 sub-catchments, precipitation amounts from 8 local monitoring sites, and precipitation chemistry from Ualand, Skreådalen and two temporary monitoring sites located within the main catchment. The examination demonstrated that the spatial variation in chemical composition was much less than the spatial variation in precipitation amount.

Marine data

Outer boundary conditions for the fjord model are based on the Coastal Monitoring data from the station Lista **(**58°01'N; 6°32'E; about 60 km SE of the Egersund estuary**)** for the years 1990 to 2003, sampled more or less regularly once a month (Moy, 2004). The model needs boundary depth profiles for salinity, temperature, oxygen, total bio-available phosphorus and nitrogen and silicate. Distributions of nutrients in different compartments (plankton, dead organic matter, dissolved nutrients) are determined by the model by analogy to the distribution within the model area, assuming

that the same biological processes take place outside the boundary as within the model area. The observation data are used to set up a seasonal two-layer statistical description, with monthly means and standard deviation for short-term variation of concentrations and depth and thickness of the pyknocline (layer showing the highest density gradient). This statistical model is used to create boundary conditions by interpolating in time and depth, applying random fluctuations in accordance with the variation in the data, assuming a reasonable time constant of about 1 week for the short-term variations.

There are no time series of hydro-chemical data available for the Egersund estuary. A one-day cruise was conducted on 28 December 2003 to obtain basic data for the model calibration. Depth profiles of salinity, temperature, fluorescence and turbidity were measured at 10 stations throughout the estuary, and water samples were taken near the surface for analysis of total phosphorus and phosphate, total nitrogen and nitrate and silicate. The river runoff was 230 $m^3 s^{-1}$ on the date of observations, and had been 160 and 270 $m^3 s^{-1}$ on the two previous days. The innermost part of the estuary (basin 1) had pure freshwater down to the maximum measured depth at 6 m, while the remaining estuary was strongly stratified with the surface layer increasing in salinity and decreasing in thickness outward through the estuary (Figure 21).

2.4 Scenarios

Simulated vs. observed climate 1980-99 (control period)
Temperature and precipitation data from HIRHAM both for the control period and the scenario periods are interpolated to the locations of the selected stations (Figure 1) and adjusted to be representative locally. The control run is, as stated above, the model's realisation of the present climate. The statistics of T and P observations are thus comparable with results from the control period. The differences in mean monthly temperature (Figure 11) and mean monthly standard deviation (Figure 12) based on daily values at the selected stations show that there is almost perfect agreement for both the MPI model and the Hadley model. For precipitation, the differences between the observed data and the two control runs are larger even though the seasonal pattern are rather well maintained (Figure 13), and the mean monthly standard deviation based on daily precipitation values also show rather good agreement (Figure 14). The frequency distribution of daily observed precipitation data at the selected stations (Table 3) was largely maintained in the control runs (Figure 15).

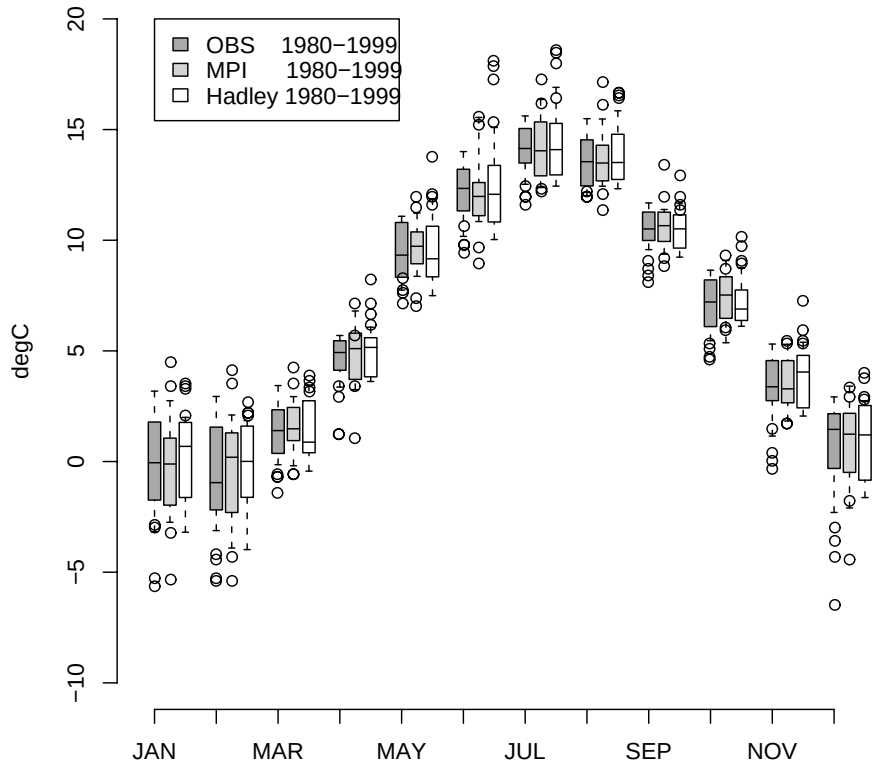

Figure 11. Boxplots of mean monthly temperatures at the station 43500 Ualand 1980-1999 for observations (OBS), the MPI run and the Hadley run. The boxes denote the 25, 50 and 75 percentiles of the monthly data. The lower and upper whiskers define the 10 and 90 percentiles, respectively.

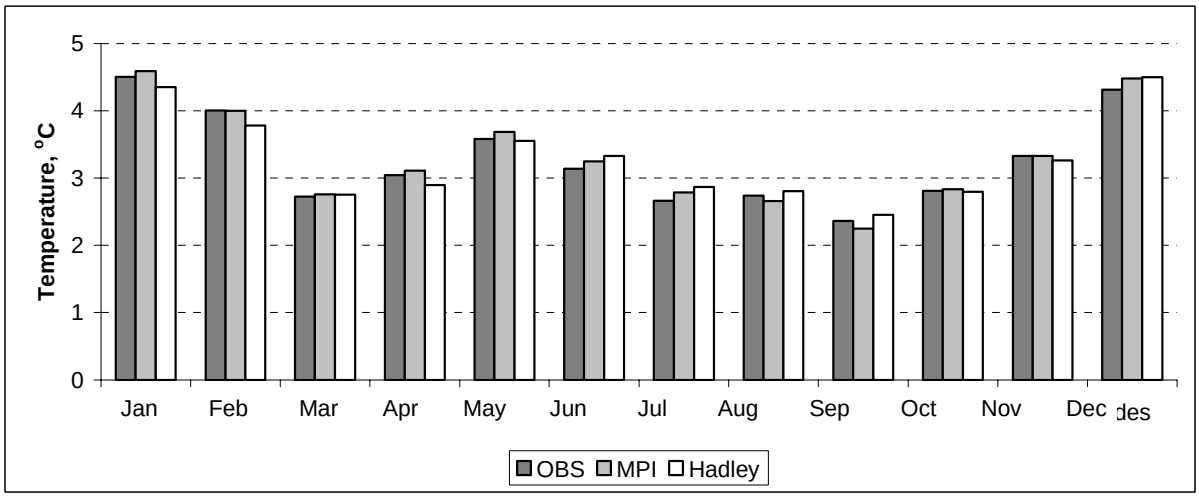

Figure 12. Mean monthly standard deviation based on daily temperature values at station 43500 Helleland 1980-99 for observations (OBS), the MPI run and the Hadley run.

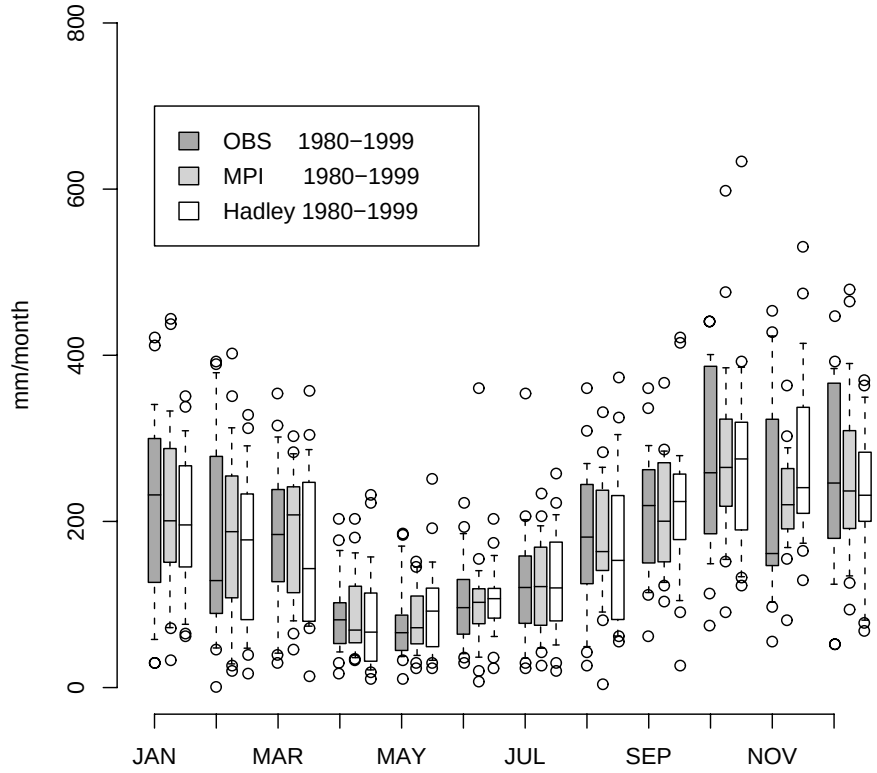

Figure 13. Boxplot of mean monthly precipitation values at the station 43450 Helleland 1980-1999 for observations (OBS), the MPI run and the Hadley run. The boxes denote the 25, 50 and 75 percentiles of the monthly data. The lower and upper whiskers define the 10 and 90 percentiles, respectively.

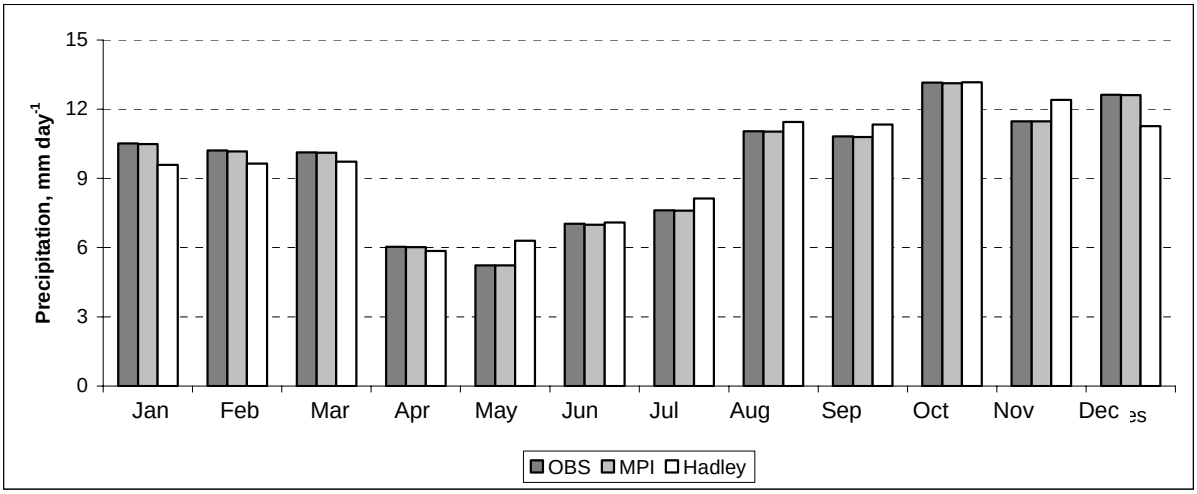

Figure 14. Mean monthly standard deviation based on daily precipitation values at station 43450 Helleland 1980-99 for observations (OBS), the MPI run and the Hadley run.

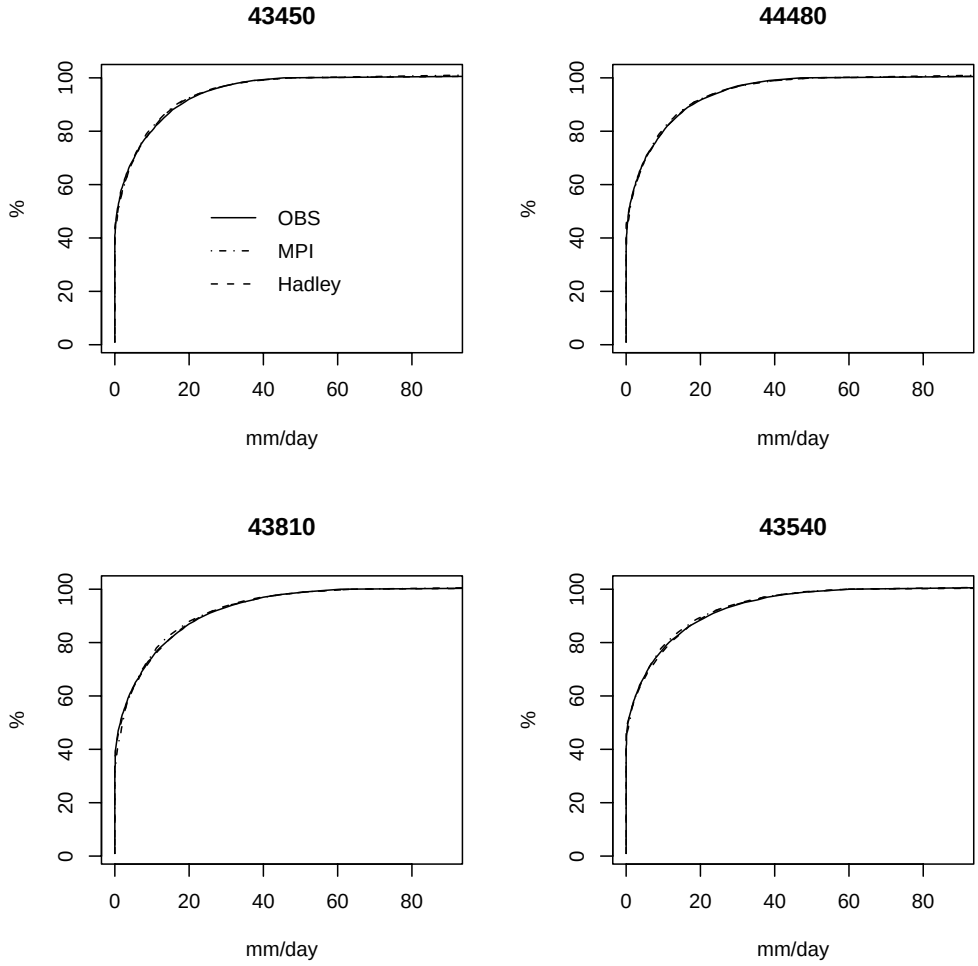

Figure 15. Frequency distribution of daily data for the control period for the selected precipitation stations (Table 3).

Future projections (2030-49 and 2080-99)
For the Bjerkreim area, the projected change in temperature differs substantially between the two model runs. The cumulative distribution curve of daily temperature values for the control period (represented by observations) and the two scenarios show that the MPI model projects a temperature increase especially during winter, spring and autumn (Figure 16). With the Hadley scenario the projected temperature increase is larger, partly because Hadley A2 entails a longer scenario period, but also because A2 is a more radical emission scenario than IS92a.

The cumulative distribution curves of daily precipitation (Figure 17) and monthly precipitation (Figure 18) show that the MPI scenario projects an increase in winter, summer and autumn. The Hadley scenario, on the other hand, projects an increase in winter precipitation, no marked change during spring and a decrease in summer and autumn precipitation.

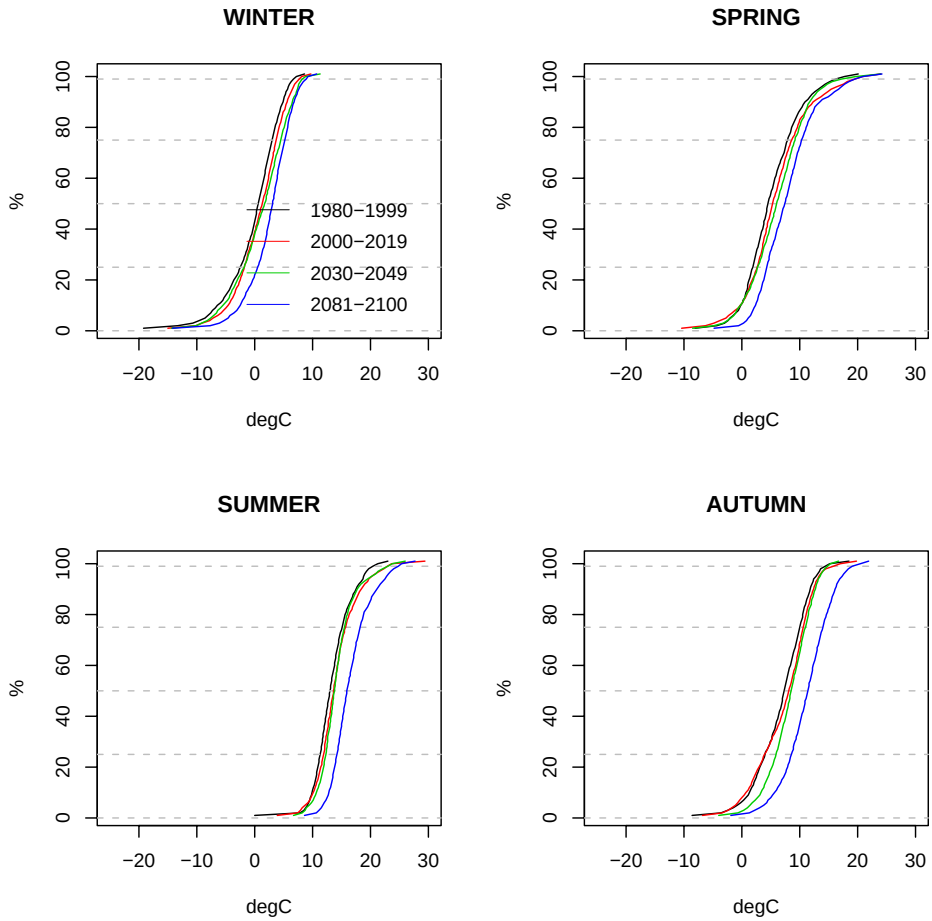

Figure 16. Frequency distribution of daily temperature values at the station 43500 Ualand 1980-1999 (here represented by observations) and the scenario periods 2030-2049 (MPI) and 2081-2100 (Hadley).

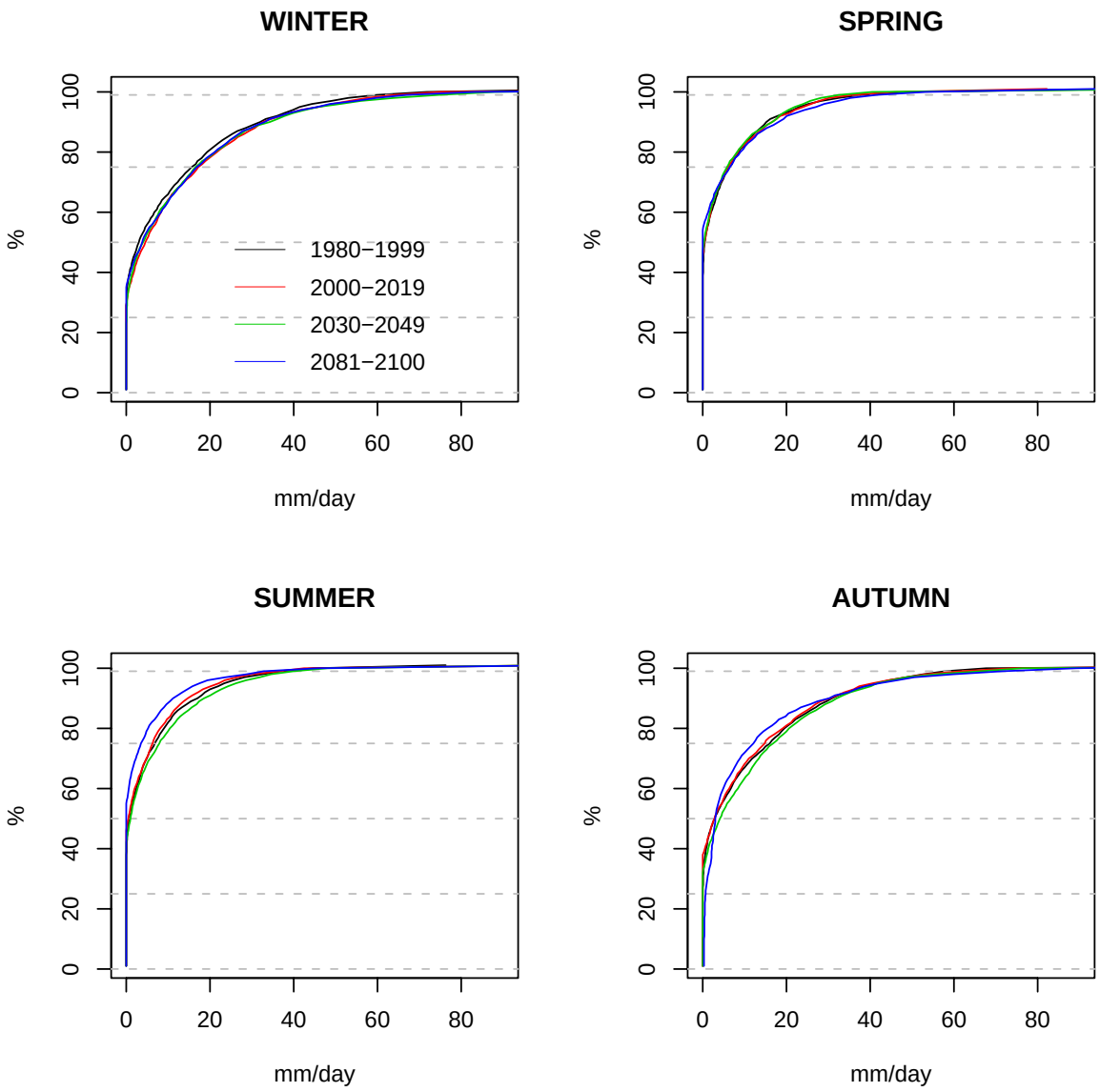

Figure 17. Frequency distribution of daily precipitation at station 43810 Maudal for the control period 1980-1999 and the scenario periods 2030-2049 (MPI) and 2081-2100 (Hadley). All precipitation stations in Table 3 showed the similar patterns.

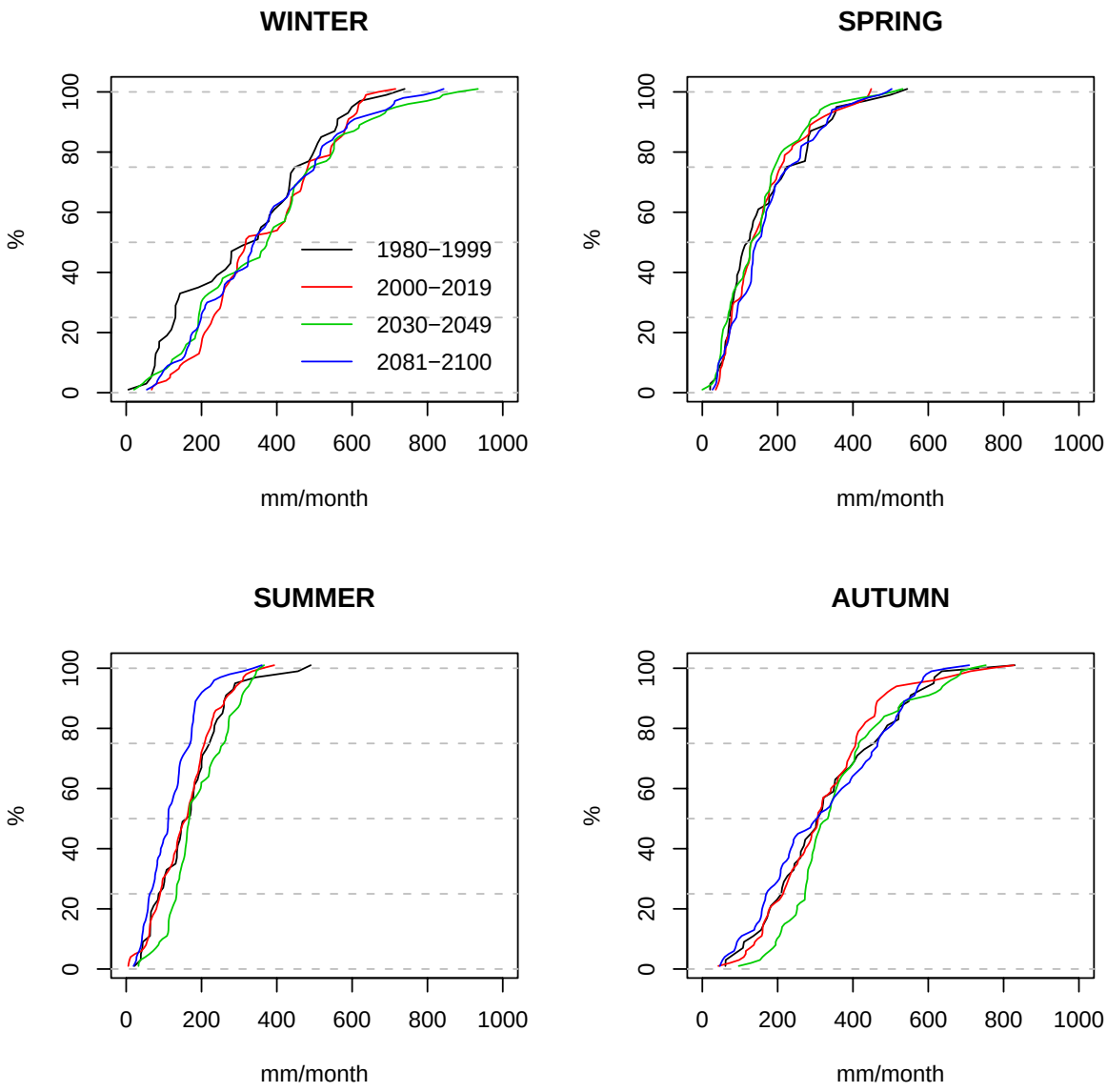

Figure 18. Frequency distribution of monthly precipitation at station 43810 Maudal for the control period 1980-1999 and the scenario periods 2030-2049 (MPI) and 2081-2100 (Hadley). All precipitation stations in Table 3 showed the similar patterns.

Deposition scenarios

Both the future scenarios (2030-2049 and 2080-2099) include full implementation of the current legislation (CLE) for future emissions and deposition of N in Europe. The CLE scenario includes the obligations agreed within the multi-pollutant, multi-effect protocol signed in Gothenburg in 1999 (UN/ECE 2002; Bull *et al.* 2001) and the limits set by the National Emission Ceilings (NEC) directive that has been adopted by the European Union. The CLE N deposition estimate was derived from a gridded dataset (150x150 km) generated by EMEP and IIASA (Schöpp *et al.* 2003). For the Bjerkreim area, this implies a reduction of the N deposition by about 35% relative to the levels in 1990.

2.5 Calibration of the effect models

HBV
None of the five precipitation stations in the Bjerkreim area are located within any of the small catchments. The Øygard catchment is located more or less in equidistant to the precipitation stations, and thus the P stations were evenly weighted. For the Svela and Apeland catchment the P station closest to catchment was set to have the strongest influence. For the sub-basins 1-6 the precipitation stations were weighted according to the Thiessen polygon method (Shaw 1994) (Table 4).

Table 4. Weight of precipitation stations in the HBV model for the 3 small catchments and 7 sub-basins in the Bjerkreim river basin (Figure 1).

Catchment	Precipitation station				
	43450	43540	43810	44480	44960
Øygard	0.33	0.34		0.33	
Svela	0.30	0.30		0.40	
Apeland	0.60	0.20		0.20	
Sub-basin 1		0.10	0.90		
Sub-basin 2		0.10	0.10	0.30	0.50
Sub-basin 3		0.60	0.30	0.10	
Sub-basin 4	0.10	0.10		0.80	
Sub-basin 5a	0.10	0.60	0.30		
Sub-basin 5b	0.80	0.10		0.10	
Sub-basin 6	0.90			0.10	

Daily observed discharge for Øygard 1993-1999, Svela 1993-1995 and Apeland 1993-1995 were used in the calibration of the HBV model for the small catchments. Scaled series of observed daily discharge at Gjedlakeiv for 1980-1999 were used for calibration and verification of the HVB model for the seven sub-basins.

Approximately 10 free parameters in the HBV model must be determined by calibration. In this study manual calibration was conducted by means of several single simulations and visual inspection of hydrograph plots. The model performance was evaluated on the basis of the Nash–Sutcliffe efficiency criterion E. E is a standardised version of the squared discharge simulation errors, with 1.0 corresponding to perfect fit. Acceptable values for hydrological model calibrations are normally within the range of 0.6-0.9 for medium-to-large sized catchments (Killingtveit and Sælthun 1995). Also the cumulative difference in simulated runoff and observed runoff was evaluated during the calibration process.

In a Nordic hydrological regime, calibration should ideally be based on five years of complete observations and supplemented with five additional years for testing the calibration (Killingtveit & Sælthun 1995). This requirement for fairly long data series is triggered by the snow melt submodel, as there is ususally only one independent major snowmelt event per year. The dynamic part of the model can be calibrated on shorter data series. Here only three years of runoff data were available for the small catchments. As snowmelt is of less important in this catchment, this is considered sufficent for calibration. For Øygard seven years of successive data (1993-1999) for the relevant time period were available. The HBV model was first set up for the Øygard catchment using recommended starting values for model parameters given in (Sælthun 1996) and the observed runoff for Øygard. A comparison of measured precipitation with measured runoff indicated, however, that the observed runoff for 1995 showed a volumetric problem probably caused by instrument malfunction during autumn 1995. As a consequence, the model was calibrated with emphasis on 1993-1994. The model was then verified by running the model for the period 1996-1999 to make sure that the model worked well outside the calibration period. Next the HBV model was set up for the other two small catchments, Svela and Apeland, and calibrated with measured runoff (1993-1995) for the respective

catchments. The observed Svela series displays a well defined volumetric error for autumn of 1994, so this period was taken out of the calculations for the E value.

For the seven sub-basins no runoff data were available for calibration so a regional parameter set was applied for the free parameters. The regional parameter set was based on the Øygard parameter set, taken to be the most representative for the whole Bjerkreim basin based on characteristics given in Table 1. Also routing through lakes in the sub-basins was included in the HBV model for these basins.

The sub-basins' simulated runoff series were checked against the area-weighted measured runoff for Gjedlakleiv (639 km^2). After running the HBV model for all the sub-basins the simulated runoff for the respective sub-basins were accumulated to give the total runoff for the Bjerkreim catchment (685 km^2). Again, this accumulated runoff series was checked against the area-weighted Gjedlakleiv runoff and the E value was calculated for the accumulated simulated series against the up-scaled Gjeldakleiv runoff series. Some systematic deviations can be identified when comparing the simulated and observed series for the total catchment, for instance a slight underestimation of the spring flood. Fine tuning of the model has not been considered necessary, as the main purpose of the model is to describe the main characteristics of changes in total and seasonal runoff caused by climate change.

After calibration the HBV model were run for the different catchments for the periods 1980-1999 with observed series of P and T as input, 1980-2049 with MPI P and T series as input, 1980-1999 with Hadley control P and T series as input and 2071-2100 with Hadley scenario P and T series as input.

MAGIC

MAGIC was calibrated to the two small catchments Øygard and Svela with annual time step. Precipitation amounts were taken from the output of the HBV simulations. Concentrations of N in deposition (wet and dry) were estimated from measurements at the NILU monitoring stations Ualand (data for 1993-99) and Skreådalen (data for 1974-2003) (Aas *et al.* 2004). The data were scaled using input-output budgets for S at Øygard and Svela, under the assumption that S input equalled S output for the 3-year calibration period 1993-95, and that the average ratios of NH_4/SO_4^* (0.77 meq/meq) and NO_3/SO_4^* (0.86 meq/meq) concentrations in precipitation measured at Ualand and Skreådalen were valid for Øygard and Svela. The asterisks denote the non-marine portion of SO_4. The long-term historical and future N deposition was taken from estimates for southern Norway derived from N emissions in Europe and the EMEP transport and deposition model (Schöpp *et al.* 2003), and scaled to the N deposition for the calibration years 1993-95 at Øygard and Svela.

The projections for the period 1996-2100 used the output from the HBV model for precipitation and discharge for the two scenarios MPI and Hadley. The discharge data were used directly in MAGIC. The 28-year record of precipitation amount and N deposition at Skreådalen station (Aas *et al.* 2004) shows a linear relationship between N deposition and precipitation amount (Figure 19). The changes in precipitation amount for the two scenarios were thus also used to change the N deposition in the future. This was combined with the current legislation scenario (CLE) for future emissions and deposition of N in Europe. The MPI scenario indicates increased precipitation, which thus will offset somewhat the decrease in N deposition as a result of the CLE.

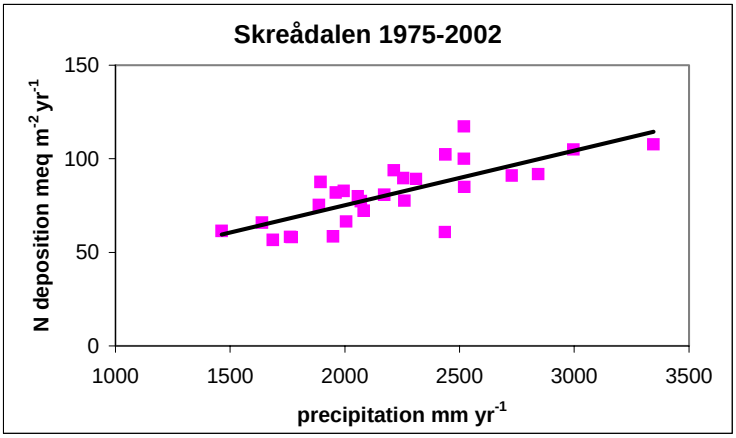

Figure 19. Relationship between annual N deposition and precipitation amount measured at Skreådalen, 1975-2002 (data from Aas *et al.* 2004). Linear regression r^2=0.57, p<0.001.

Both the MPI and the Hadley scenarios project future increase in mean annual temperature. With respect to N processes in MAGIC the increase in temperature was assumed to increase the decomposition of organic matter in the soil. This assumption rests on the results from the whole-ecosystem climate change experiment of CLIMEX, in which the temperature (and CO_2 concentration in air) was increased by 3.7 ^oC above ambient to an entire forested headwater catchment at Risdalsheia, southernmost Norway. The CLIMEX catchment responded with increased mineralisation of N in the soil and increased NO_3 concentrations in runoff (Van Breemen *et al.* 1998). A MAGIC application to these CLIMEX data indicated that these responses could be simulated by an annual net loss of soil C due to decomposition of organic matter of 1 molC m^{-2} yr^{-1} (Wright *et al.* 1998a). The C is lost to the atmosphere as CO_2, and the C/N ratio of the remaining organic matter decreases. The soil thus progresses more rapidly towards N saturation. For simulating the effect of the temperature changes of the MPI and Hadley scenarios, the temperature change was assumed to increase smoothly from the control period 1980-99 to the evaluation period (2030-49 MPI; 2080-99 Hadley). The change in decomposition rate was scaled to the temperature change (Figure 20).

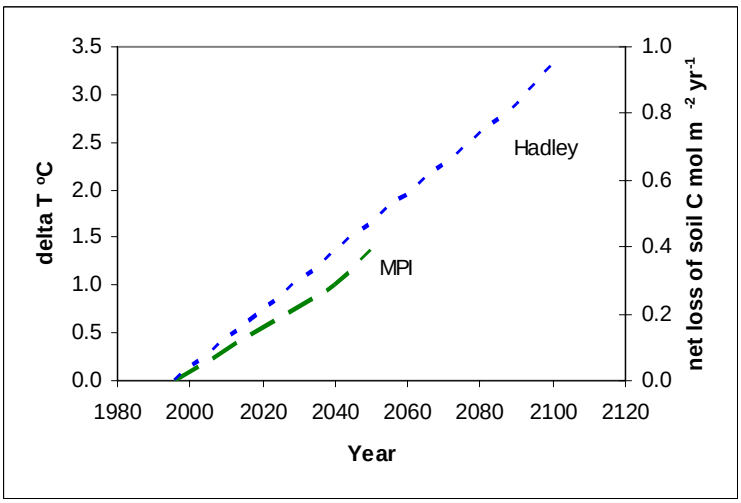

Figure 20. Changes in temperature and annual net loss of soil C by decomposition of soil organic matter used in MAGIC to simulate the effects of the two scenarios MPI and Hadley.

Soil data came from samples collected during 2000 at Øygard (J. Mulder unpublished) and 1995 at Svela (Mulder *et al.* 1997). Lake data came from (Sjøeng 1998). Runoff chemistry data were derived from samples collected in 1993-95 at the weirs at Svela and Øygard (Kaste *et al.* 1997). Data for subsequent years at Øygard came from the monitoring programme (SFT 2004).

The calibrations assumed 100% nitrification in both soil and surface water, as the observed concentrations of NH_4 in streamwater and lakewater at these sites is seldom greater than 1 µeq L^{-1}. Net uptake of N in vegetation was assumed to be matched by litterfall (thus no increase of N in biomass over time). This assumption is reasonable for the Øygard catchment, as here there is no removal of biomass. For Svela this assumption entails no further management of the existing forest, and that the future increase in N stored in biomass (mostly stems of the trees) is negligible. Denitrification was assumed negligible. Finally the amount of C stored in the active soil organic matter pool was assumed to be constant over time, except for the effects of climate change in the future (Table 7). The calibration required only the fitting of the C/N curve to the observed fluxes and pools (Figure 6). The C/N_{up} was adjusted such that the simulated NO_3 concentration in streamwater matched the observed for the years 1993-95, and the range (distance between C/N_{up} and C/N_{lo}) was assumed to be 11.

INCA-N

INCA-N, version 1.7 has previously been calibrated to the Bjerkreim river basin 1993-95 (Kaste 2004). Model calibration was carried out as recommended by Wade *et al.* (2002): After including the appropriate initial values, INCA-N was set up to simulate the hydrological parameters both in terms of dynamics and absolute flow before any parameters controlling N storage, transformations or transport were adjusted. Secondly, the parameters controlling terrestrial and in-stream N transformation rates were adjusted such that annual process loads were within the ranges reported in the literature and a reasonable match between simulated and observed streamwater NO_3 concentrations was obtained.

In the relatively large and complex Bjerkreim river basin, the model was first calibrated for three small and relatively homogenous catchments Svela (61% forest), Øygard (83% heath and mountains), and Apeland (33% pasture and arable land). When scaling up to the entire Bjerkreim catchment (685 km^2), the main river was first divided into seven reaches (Figure 1). Hydrological time series (SMD, HER, AT, P) were then assigned to each of the individual reaches, and hydrological parameters such as storage volumes and velocity/flow relationships were calibrated. Further, N process parameters from the small catchments were applied to the corresponding land cover classes in the main basin.

The most recent version of INCA-N (v.1.9) was used for this study. Owing to some structural changes introduced by this model version and also the new HBV-based hydrological input data, the model was re-calibrated with the original 1993-95 parameter sets plus some additional parameters required by the new version of the model (see full parameter file Appendix A1). Among these the temperature response parameters, Q_{10} and Q_{10bas}, that were assigned to each of the N processes included in the model (Figure 9).

The long-term balance between N accumulation and release processes were simulated by applying soil carbon to nitrogen dynamics from the MAGIC model (Figure 6). More specifically, N immobilisation rates during the periods 1980-99, 2030-49 and 2080-99 were adjusted in INCA-N to match N retention time series generated by the MAGIC model.

NIVA Fjord Model

The estuary model is run for the different climate scenario output data from INCA-N. The scenarios differ only with respect to water flow and nitrogen runoff as modeled by the INCA-N model, and in addition changes in silicate runoff related to changes in the water flow as described above. The seaward boundary conditions and the meteorological data are the same in all scenarios. Thus, the estuary model scenario simulations only include changes in water flow and associated changes in nitrogen and silicate. The direct effect of changed weather conditions on the estuary (light, temperature, wind) or changed conditions in the coastal waters outside is outside the scope of this study, which focuses on the linkage through the model chain.

The fjord model was set up with the model area in Figure 2 divided in a sequence of 5 connected basins, with basin 1 as the innermost part, and basin 4 and 5 representing the main outer part of the estuary. An initial inspection of results showed that a large outer 'virtual' basin 6 outside the model area was needed to get stable and realistic results in the 5 proper model basins. The small basins of the Bjerkreim estuary have too short residence time for the estuary to be controlled by internal processes; it depends on influx of plankton biomass from the coastal waters outside. The virtual basin 6, with surface area set to 100 km^2, provided this stability to the model.

Figure 21 and Figure 22 show modeled salinities extracted from the time series for situations where runoff was between 200 and 250 m^3/s. The general features of the observed stratification were captured fairly well by the model, even if the stratification given by the model is too sharp.

The volume of the surface layer, down to about 5 m depth, is about $18 \cdot 10^6$ m^3. With an average salinity above the pycnocline in the range 5-10‰, and a salinity of about 30‰ in the probable inflow layer below the pycnocline, the residence time of the surface layer at this time can be estimated to be in the range about 15-20 hours.

Average daily freshwater runoff values vary from 2 to 400 $m^3\ s^{-1}$. If freshwater is contained in a surface layer about 4 m thick or a volume of about $15 \cdot 10^6$ m^3 with salinity around 5‰, the residence time within the estuary would be about 10 hours for a high runoff of 400 m^3/s and about 40 hours for a runoff of about 100 m^3/s. At low runoff ($2m^3/s$), assuming a surface layer of salinity 15 and depth 1 m, the residence time of the surface layer should be on the order of 10 days.

The monthly averages of observed particulate carbon concentrations in the surface layer (0-5 m depth) of the coastal monitoring station at Lista are typically around 180-240 µg C L^{-1} from April to October and 40-120 µg C L^{-1} in winter. The modelled particulate carbon concentrations in surface layers in the estuary have a seasonal peak with values 120-200 µg C L^{-1} lasting from May to August, with a more gradual reduction through September and October to low levels of about 10 µg C L^{-1}. The larger virtual basin that is supposed to represent roughly the coastal current has higher peak values 280-400 µg C L^{-1} but with about the same seasonal pattern as the other model basins. The Bjerkreim model setup only includes biomass produced within the model area, and ignores external input of detritus with the river or in the coastal current, so it is reasonable that results differ from observations in this way.

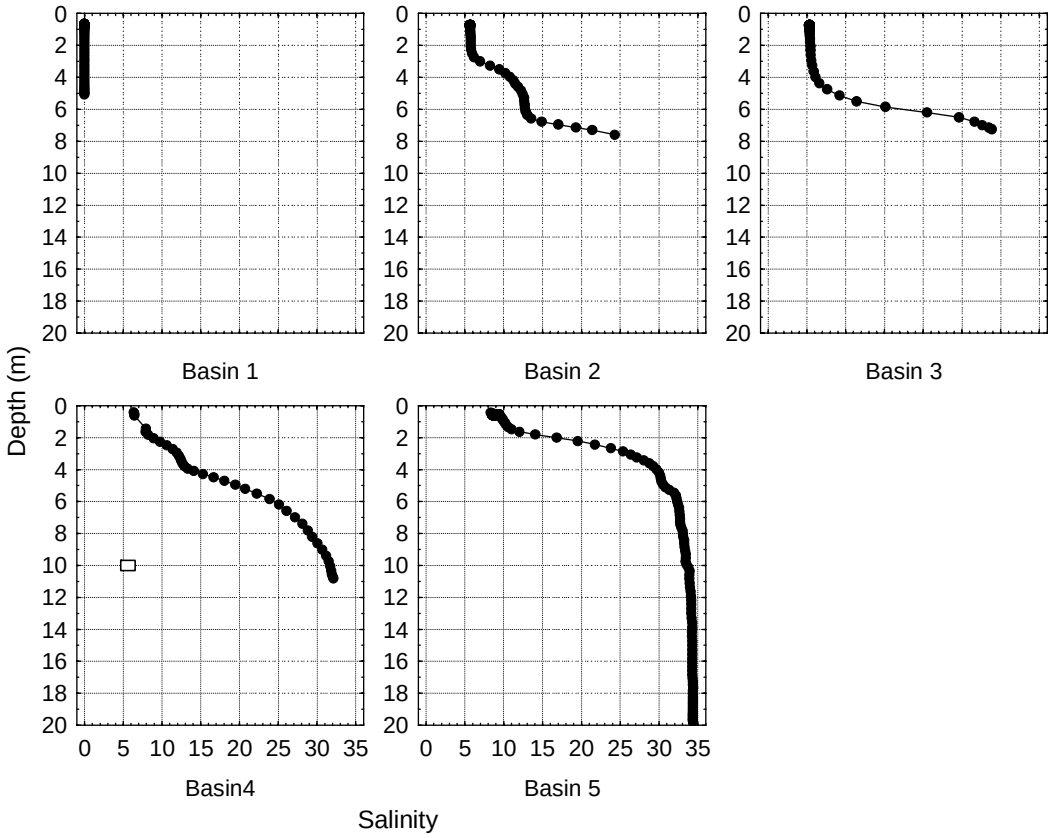

Figure 21. Observed salinity (‰) in the Egersund estuary, 28 December 2003.

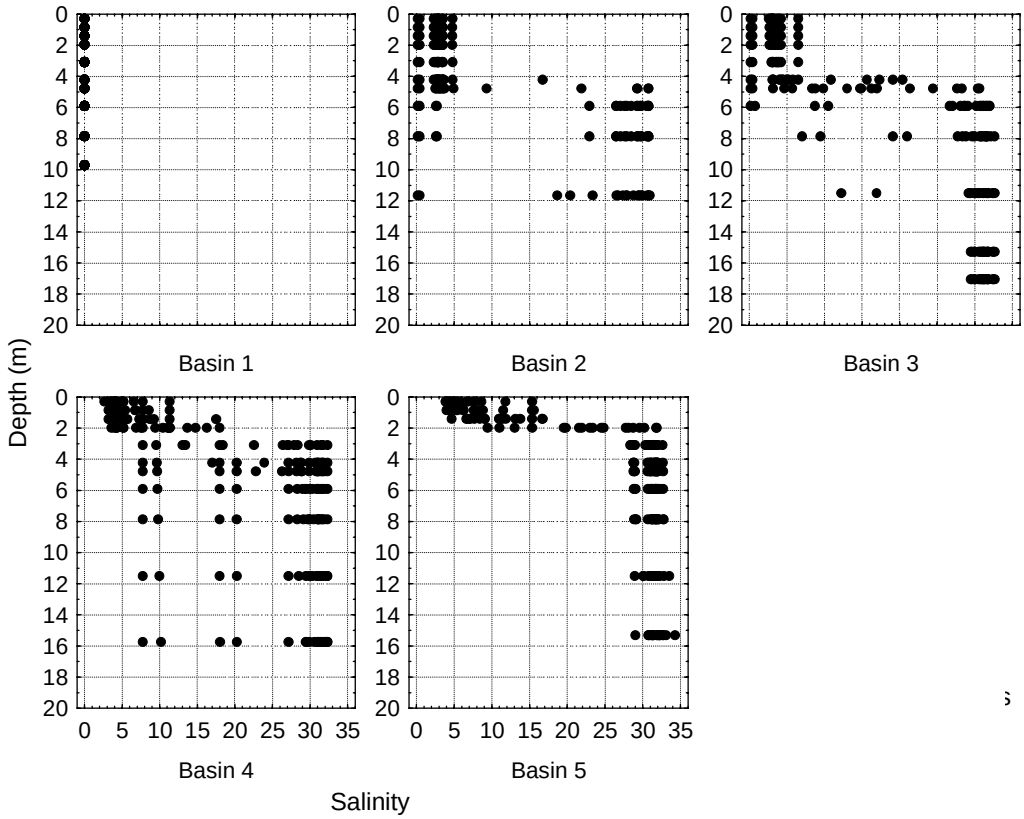

Figure 22. Modeled salinities (‰) in runoff situations similar to the situation observed 28 December 2003 (Figure 21).

3. Results

3.1 Hydrology (HBV model)

Calibration results
The model performance was evaluated on the basis of the Nash–Sutcliffe efficiency criterion (E). The E values for the HBV simulations was generally markedly lower for the small catchments, which had only short runoff series with variable quality for calibration, than for the medium-to-large sized basins. Svela is a very small and steep catchment with extremely quick response. The E measure is very sensitive to timing problems in quick floods (flood peak simulated one day early or late), which often occurs in the simulations from this catchment. When calculated on running three-day means for Svela, the E value increased to 0.40. When leaving out the erroneous observed values of autumn of 1994, the E value increased further to 0.62. These issues taken into consideration, the Svela simulation results were considered acceptable.

The accumulated runoff from the seven sub-basins constituting the Bjerkreim runoff has not been calibrated against observed runoff, but corresponds well with the upscaled Gjedlakleiv runoff series. The major systematic difference is an underestimation of the spring runoff and an overestimation of the late autumn runoff in the simulated series (Figure 23). A probable explanation is that the snow accumulation is underestimated in the model. The reason for this is either that the temperature lapse rate is underestimated or that the temperature station is too close to the coast to be representative for the inland/highland sub-basins. The model parametrisations were left unaltered.

Table 5. Calibration results from the HBV modelling. E is the Nash–Sutcliffe efficiency criterion.

Catchment	Period	E	Water balance (mm)		
			Simulated runoff	Observed runoff	Difference (%)
Øygard	1993-1995	0.47	5586	5375	+3.2 %
	1993-1994	0.56	3557	3482	+2.2 %
	1996-1999[a]	0.57	8017	8139	–1.5 %
Svela	1993-1995	0.22	3979	4300	–7.5 %[c]
	1993-1995[b]	0.29			
Apeland	1993-1995	0.59	3989	3879	+2.8 %
Bjerkreim	1980-1999	0.66	48725[d]	46727[e]	+4.3 %

[a] Verification period; [b] without Sep-Dec 1994; [c] corresponds to the deficit of autumn 1994; [d] accumulated runoff from sub-basins 1-6; [e] Gjedlakleiv up-scaled

Control period simulations
Generally the runoff simulations based on observed temperature and precipitation and on climate model outputs for the control period (1980-1999) are in good correspondence with each other and with observed runoff, measured by average monthly runoff (Figure 23 and Figure 24). There is some discrepancy between Øygard simulated and observed runoff (Figure 23), but this might be explained by statistical variations arising from the shorter length of observed data for Øygard relative to the other series.

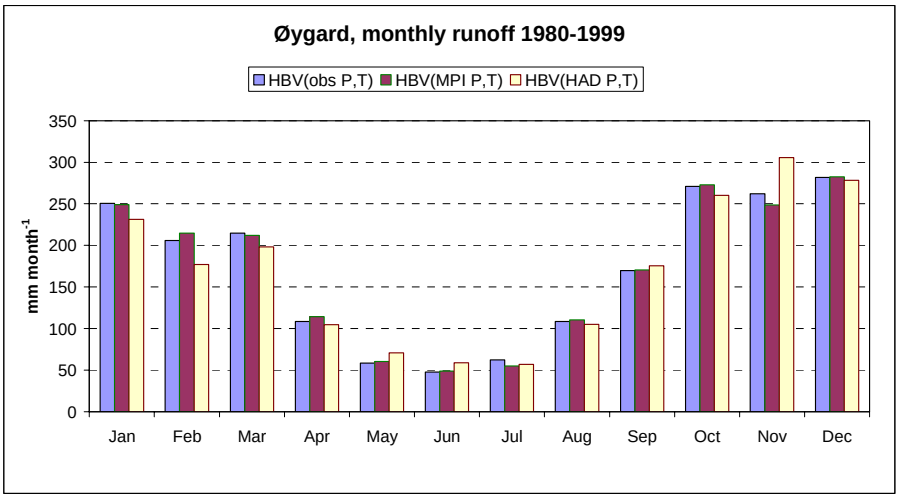

Figure 23. HBV simulations for the Øygard catchment for the control period 1980-1999.

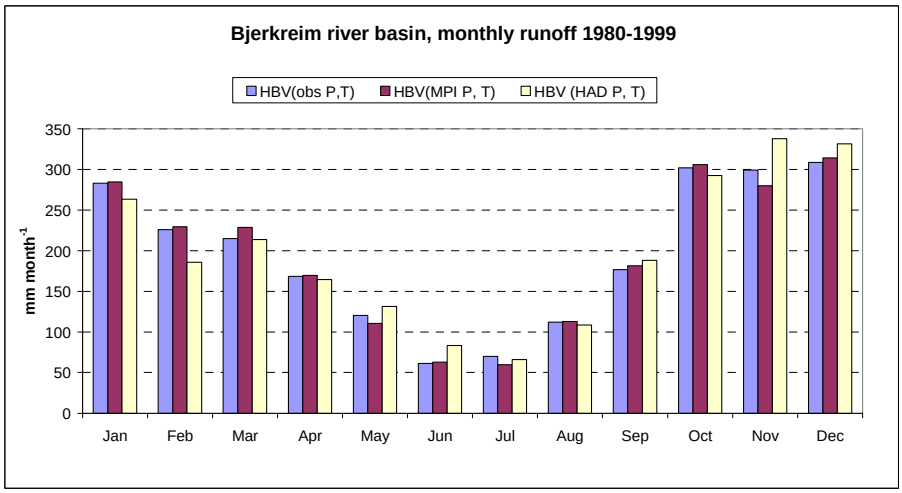

Figure 24. HBV simulations for the Bjerkreim river basin for the control period 1980-1999 based on accumulated HBV simulated runoff for the sub-basins 1-6 (Figure 1).

Scenario simulations

Runoff

The MPI scenarios show a precipitation increase of 10 per cent over the 50 year time span from 1990 to 2040. This is reflected in a runoff increase of 9 percent (**Table 6**). The seasonal pattern displays an increase in winter runoff and little change in the summer (Figure 25 and Figure 27). The temperature increase is moderate, 1^{o}C over the 50-year period, and the evapotranspiration increases only slightly.

The Hadley scenarios give completely different results. Precipitation is more or less unchanged over the 100-year period, and the temperature increases by 3 ^{o}C. The result is increased evapotranspiration and a significant reduction in runoff, approximately 10%. The seasonal change is characterized by a large reduction of runoff in late summer due to increased evapotranspiration and soil moisture deficit. There is a slight increase in winter runoff (Figure 26 and Figure 27).

Table 6. Mean annual temperature and precipitation (output from the regional downscaled AOGCMs and used as inputs to HBV) and runoff (output from HBV) for the control period 1980-99 and the assessment periods 2030-49 (MPI) and 2080-99 (Hadley) for Øygard, Svela and the Bjerkreim river basin.

T (°C)		**Øygard**			**Svela**		**Bjerkreim river basin**		
Period	OBS	MPI	Hadley	OBS	MPI	Hadley	OBS	MPI	Hadley
1980-99	5.6	5.6	5.6	5.8	5.8	5.8			
2030-49		6.6			6.8				
2080-99			8.5			8.8			
% change		+1.0	+2.9		+1.0	+3.0			
P (mm/yr)									
1980-99	2513	2519	2487	1960	1964	1945			
2030-49		2775			2168				
2080-99			2481			1944			
% change		+10%	–1%		+10%	0%			
Q (mm/yr)									
1980-99	2042	2039	2022	1456	1447	1441	2436 2336[a]	2331	2358
2030-49		2227			1578			2532	
2080-99			1888			1327			2123
% change		+9%	–8%		+9%	–9%		+9%	–10%

[a] up-scaled measured series for Gjedlakleiv

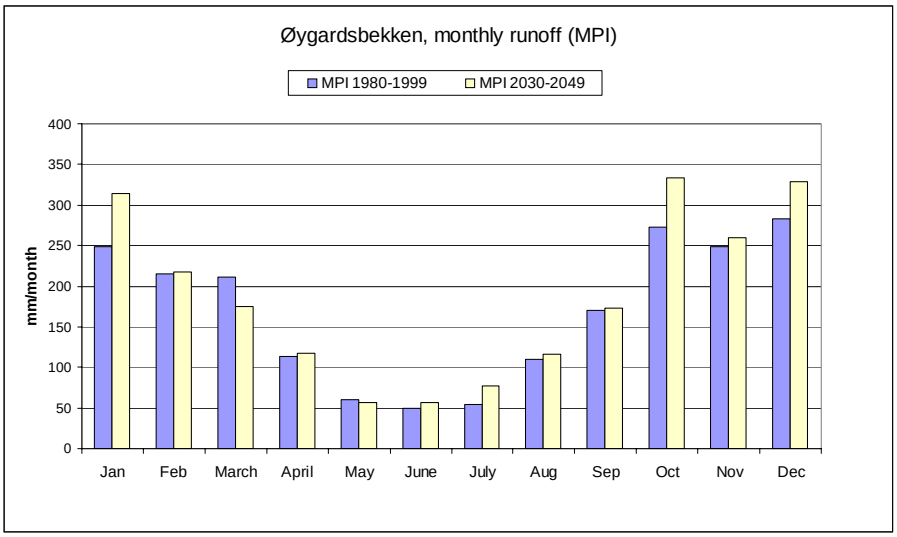

Figure 25. Monthly runoff for the Øygard catchment, simulated by HBV with the MPI scenario.

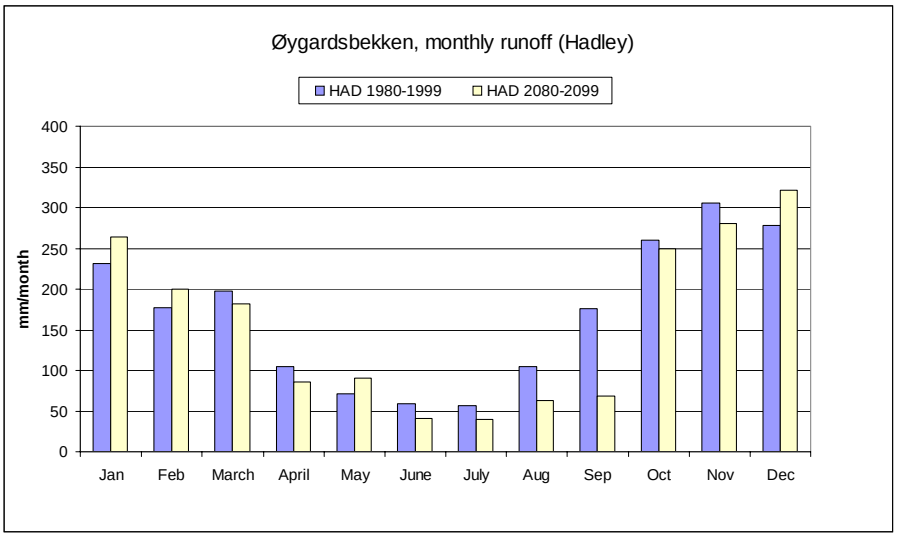

Figure 26. Monthly runoff for the Øygard catchment, simulated by HBV with the Hadley scenario.

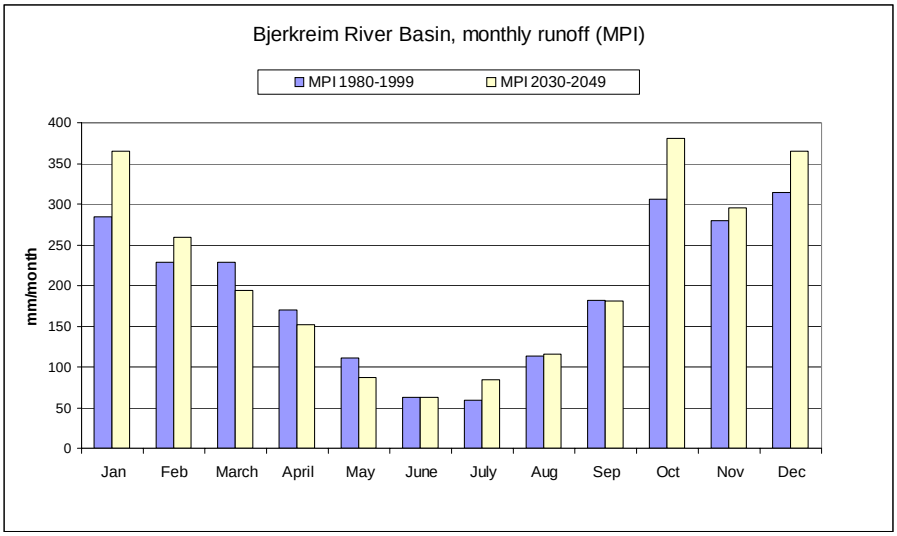

Figure 27. Monthly runoff for Bjerkreim river basin (based on accumulated simulations for sub-basins1-6). Simulated by HBV with the MPI scenario.

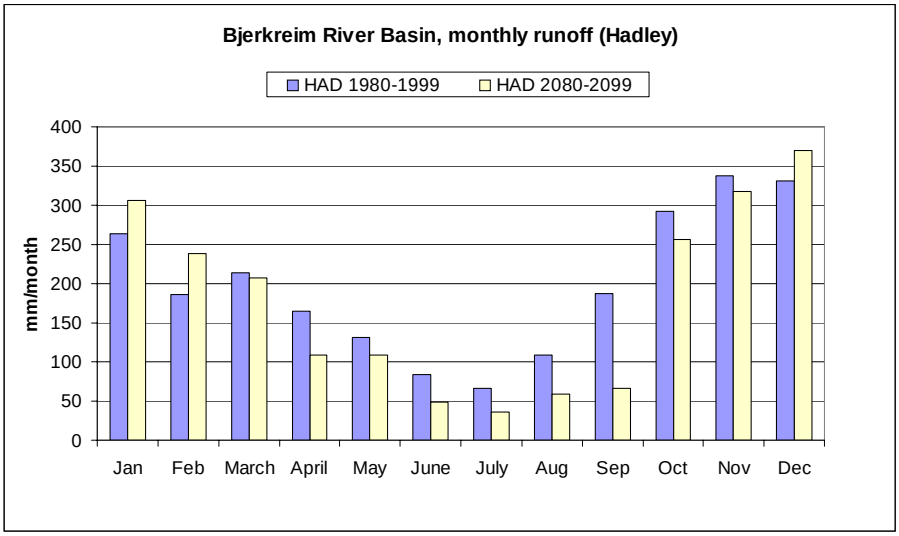

Figure 28. Monthly runoff for Bjerkreim river basin (based on accumulated simulations for sub-basins1-6). Simulated by HBV with the Hadley scenario.

Snow

The MPI and Hadley scenarios project an increase in future winter precipitation (Figure 17). With the moderate temperature change in the MPI scenario the snow accumulation changes are not dramatic at lower and intermediate altitudes as represented by the Øygard catchment (Figure 29). For highland basins like R1, which have larger and more stable snow cover during winter, the changes are more clearcut (Figure 31). Measured as number of days per year with snow cover, the MPI simulation period shows a diminishing trend from 100 days per year in 1980 to 60 days in 2049 (Figure 32). The Hadley scenario, with stable precipitation and stronger temperature increase shows a dramatic reduction of snow cover both at Øygard and in the higher R1 sub-basin (Figure 30, Figure 31).

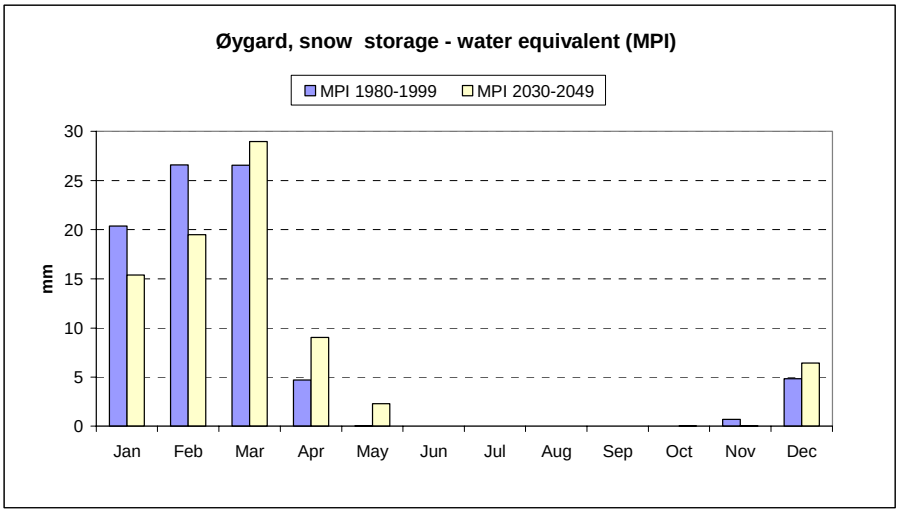

Figure 29. Snow storage in the Øygard catchment, simulated by HBV with the MPI scenario.

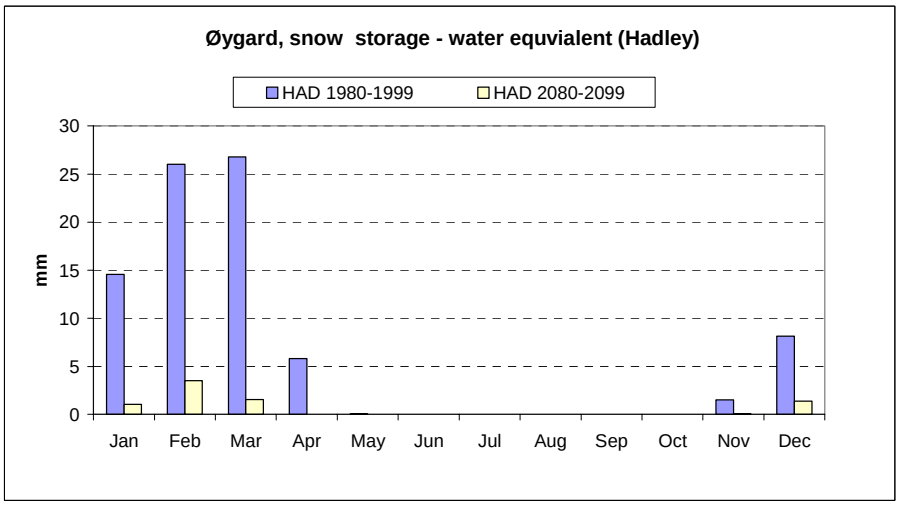

Figure 30. Snow storage in the Øygard catchment, simulated by HBV with the Hadley scenario.

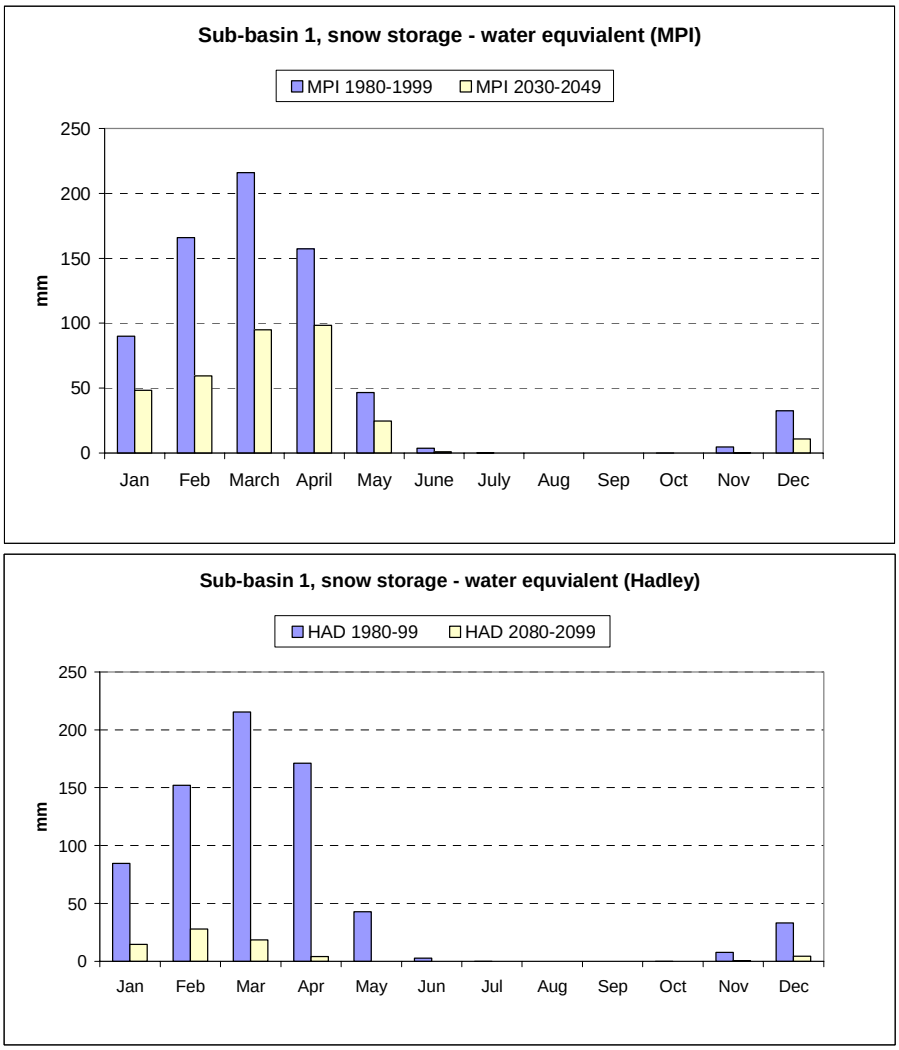

Figure 31. Snow storage in sub-basin 1, simulated by HBV with the MPI and Hadley scenarios.

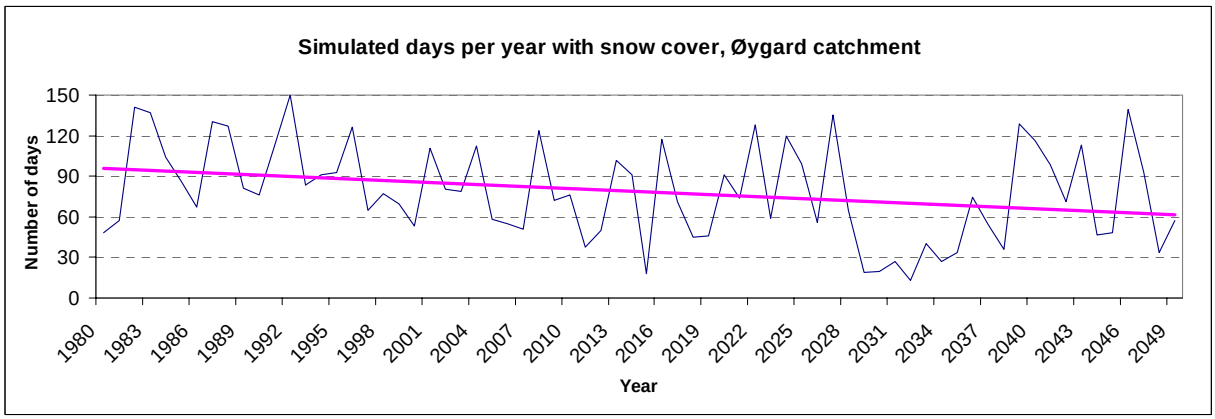

Figure 32. Days with snow in the Øygard catchment for the period 1980-2049, based on HBV simulations with the MPI scenario.

Soil Moisture Deficit (SMD)

As the summer precipitation increases in the MPI scenario, and the temperature increase is moderate, soil moisture deficit is not significantly changed in these simulations (Figure 33). The Hadley scenario, on the other hand, with reduced summer precipitation and increased temperature, produces a marked increase in soil moisture deficit in late summer (Figure 34). The increase is especially pronounced in September, when SMD is more than doubled compared to the control period.

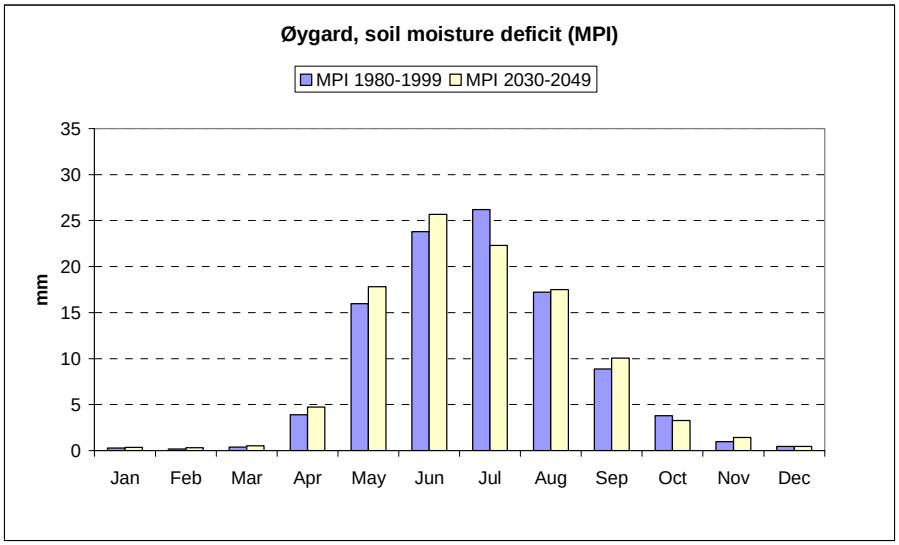

Figure 33. Soil moisture deficit for the Øygard catchment, simulated by HBV with the MPI scenario.

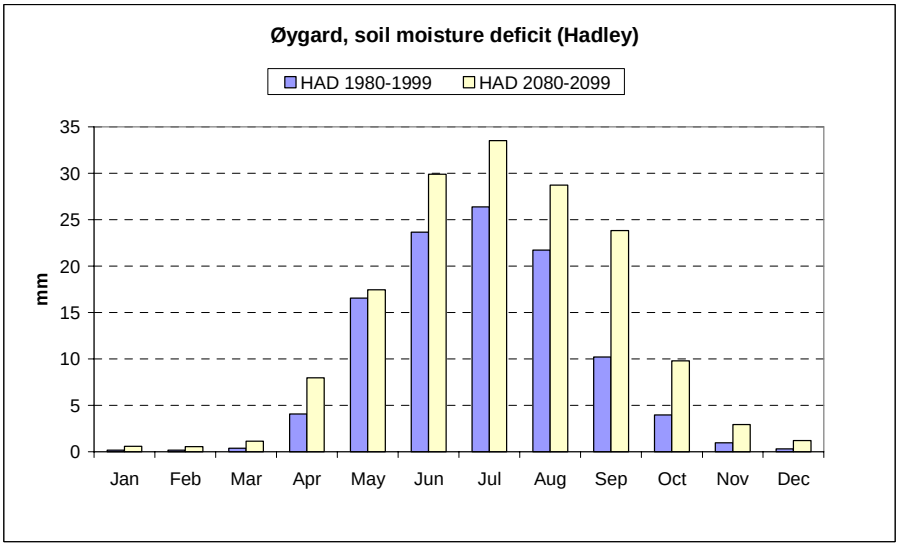

Figure 34. Soil moisture deficit for the Øygard catchment, simulated by HBV with the Hadley scenario.

3.2 Acidification history and catchment N status (MAGIC model)

Calibration results
In the calibration period 1993-95 the streams at both Øygard and Svela had significant volume-weighted mean concentrations of NO_3, 12 and 11 µeq L^{-1}, respectively. NH_4 concentrations were negligible (mean 2000-2004: <0.5 µeq L^{-1}, N=71). The N dynamics in MAGIC was calibrated to match these concentrations (Table 7, Figure 35, Figure 36).

Hindcast period 1860-1995
The assumptions in the model are such that prior to the onset of N deposition (here assumed to be year 1860) all N was retained in the ecosystems and thus concentrations of NO_3 in the streams were near zero. During the hindcast period (1860-1995) N deposition in southern Norway gradually increased (Schöpp *et al.* 2003). The model indicates that as the catchment soils became increasingly saturated with N, an increasing fraction of the N deposition was lost in the form of NO_3 to runoff (Figure 35). By the year 1995 N saturation had proceeded to the point at which 15% and 5% was lost at Øygard and Svela, respectively.

Table 7. MAGIC. Measured, estimated and calibrated parameters for Øygard and Svela catchments. N.A. = not applicable.

	Units	Øygard	Svela
Deposition			
Precipitation amount 1993-95	mm yr^{-1}	2310	1797
Precipitation amount 1980-99	mm yr^{-1}	2513	1944
NH_4 1993-95	meq m^{-2} yr^{-1}	60	35
NO_3 1993-95	meq m^{-2} yr^{-1}	72	39
Surface water			
discharge 1993-95	mm yr^{-1}	1849	1307
discharge 1980-99	mm yr^{-1}	2042	1456
NO_3 1993-95	µeq l^{-1}	12	11
lake relative area	%	7	0
lake retention time	yr	0.2	N.A.
sedimentation velocity NO_3	m yr^{-1}	5	N.A.
nitrification	%	100	100
Soil			
depth	m	0.40	0.22
porosity	fraction	0.5	0.5
bulk density	kg m^{-3}	351	294
C pool	mol m^{-2}	2574	1437
N pool	mol m^{-2}	99	76
C/N	mol mol^{-1}	25.9	18.9
nitrification	%	100	100
Calibrated parameters			
initial N pool (year 1860)	mol m^{-2}	89	71
initial C/N (year 1860)	mol mol^{-1}	28.9	20.3
C/N_{up}	mol mol	28.0	21.2
C/N_{lo}	mol mol	17.0	10.2

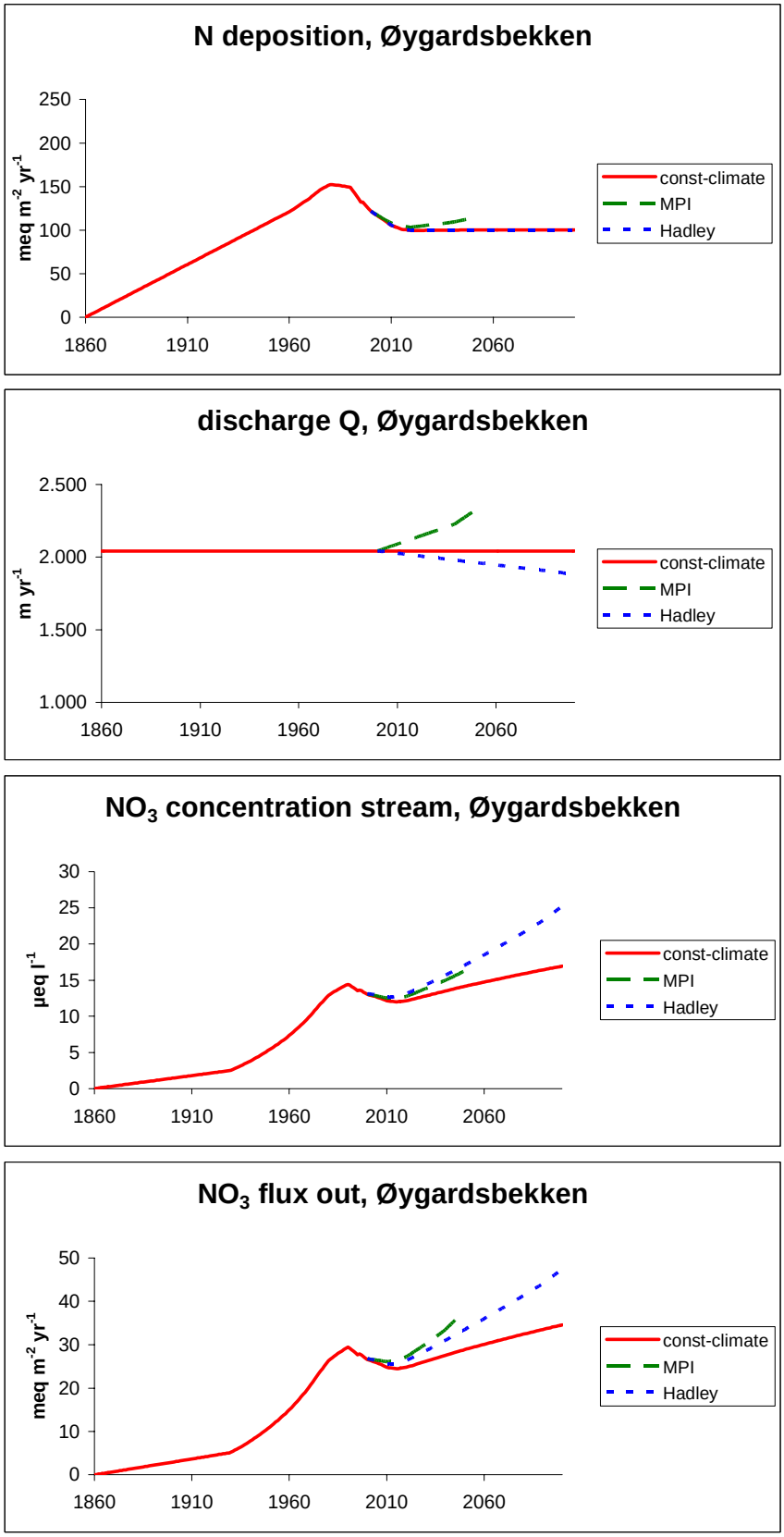

Figure 35. MAGIC simulated NO_3 concentrations and fluxes in the stream at Øygard reconstructed for the period 1860-1995 and forecast for the period 1996-2100. Also shown are inputs for N deposition derived from the AOGCMs and N emission scenarios for Europe and the discharge obtained as output from the HBV model.

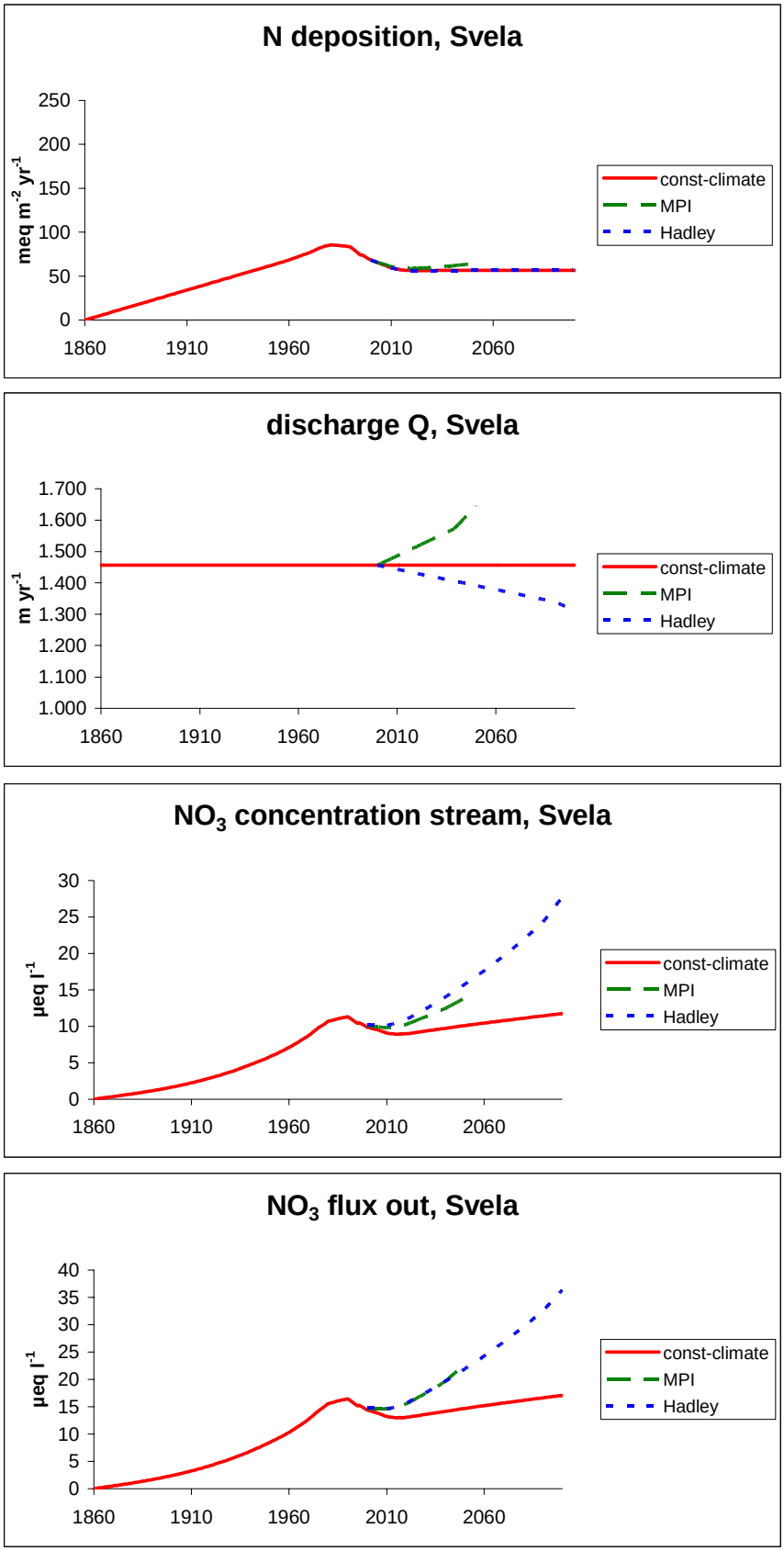

Figure 36. MAGIC simulated NO_3 concentrations and fluxes in the stream at Svela reconstructed for the period 1860-1995 and forecast for the period 1996-2100. Also shown are inputs for N deposition derived from the AOGCMs and N emission scenarios for Europe and the discharge obtained as output from the HBV model.

Forecast period 1996-2100

The CLE scenario for N deposition entails about a 35% decrease from 1990 to 2020 at both catchments (Figure 35). Of the two climate change scenarios the MPI scenario indicates an increase in precipitation and thus N deposition (cf. Figure 19), whereas the Hadley scenario indicates no change in precipitation. The two climate scenarios also differ with respect to predicted discharge; the MPI scenario entails increased discharge, while the Hadley scenario entails decreased discharge (Figure 35). Decreased discharge at constant precipitation is due to the increased evapotranspiration caused by the increase in temperature.

NO_3 concentrations in the streams are projected to increase in the future under all three scenarios (Figure 35). Under the constant climate scenario NO_3 concentrations first decline in response to the decreased N deposition, but then increase again due to progressively higher N saturation in the catchment soils. Under both of the climate change scenarios MAGIC suggests that NO_3 concentrations will increase more rapidly than under constant climate. This is due to the gradual reduction in size of the soil C pool (due to the increased decomposition in response to increased temperature). Also the flux of NO_3 is projected to increase under all three scenarios, with a greater increase given the two climate change scenarios (Figure 35).

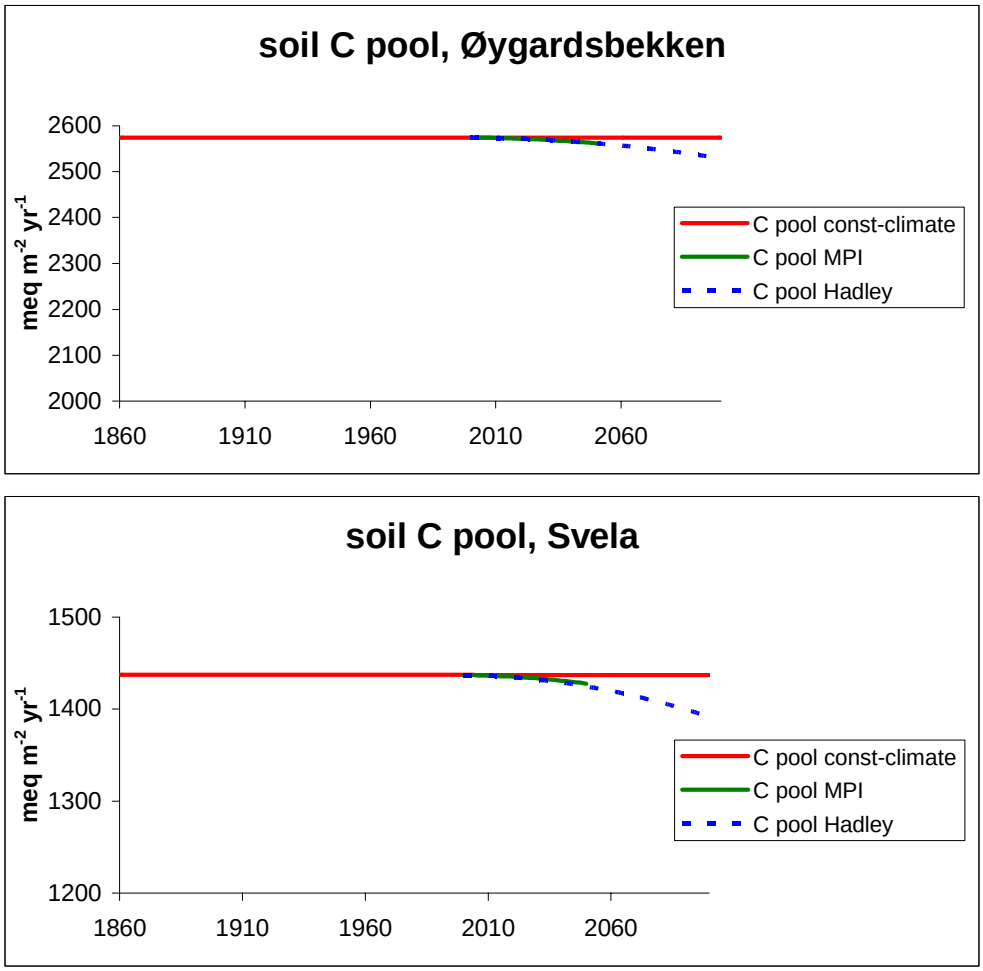

Figure 37. Projected changes in soil C pool at Øygard and Svela under scenarios of constant climate and climate change (MPI and Hadley are very similar).

Table 8. Summary of results from MAGIC at the two small sub-catchments Øygard (moorland) and Svela (forested). Mean annual N deposition, NO_3 concentration in streamwater, and NO_3 flux out for the control period 1980-99 and the assessment periods 2030-49 and 2080-99 with constant climate, the MPI scenario and the Hadley scenario.

	Øygard			Svela		
	Constant	MPI	Hadley	Constant	MPI	Hadley
N dep. (meq m^{-2} yr^{-1})						
1980-99	144	144	144	80	80	80
2030-49	100	109		56	62	
2080-99	100		100	57		57
NO_3 in stream (µeq l^{-1})						
1980-99	14	14	14	11	11	11
2030-49	13	15	16	9	12	
2080-99	16		23	11		24
N flux (meq m^{-2} yr^{-1})						
1980-99	28	28	28	16	16	16
2030-49	27	33		14	20	
2080-99	33		44	17		32

3.3 Streamwater N concentrations and fluxes (INCA-N model)

Calibration results

A former version of the INCA-N model (v. 1.7) was previously calibrated to the Bjerkreim river basin 1993-95, including the small sub-catchments Øygard and Svela (Kaste 2004). Owing to structural changes and new parameters imbedded in the new INCA version (1.9), and also the introduction of new hydrological input data generated by HBV, the model was re-calibrated on basis of the original 1993-95 parameter sets for Øygard, Svela and the Bjerkreim river outlet. The hydrological re-calibration did not lead to any major changes in the simulated discharge volumes and flow dynamics relative to the former calibration (Table 9). Mean NO_3^- concentrations were simulated well for the main river outlet, whereas the concentration levels simulated at Øygard and Svela were 10-20% higher than the observed (Figure 38). This was mainly due to higher simulated winter concentrations. The seasonal patterns in NO_3^- concentrations were reproduced fairly well at the small catchments, whereas the simulation for the main river was somewhat poorer (Figure 38). Here the seasonal pattern is weaker and complicated by numerous anthropogenic N sources and also dampening effects caused by large lakes in the basin.

Table 9. Calibration results 1993-95 with INCA-N v. 1.9. Results from the former INCA-N v. 1.7 calibrations are in parentheses. Temporal patterns are investigated by simple linear regression.

	Streamwater discharge		NO_3^- concentration	
	Mean (sim./obs. ratio)	Temporal pattern (r^2)	Mean (sim./obs. ratio)	Temporal pattern (r^2)
Bjerkreim river basin	0.99 (1.02)	0.66 (0.73)	1.00 (1.02)	0.17 (0.26)
Svela catchment	0.95 (1.11)	0.46 (0.47)	1.23 (1.00)	0.67 (0.68)
Øygard catchment	1.06 (1.02)	0.74 (0.66)	1.08 (1.03)	0.43 (0.46)

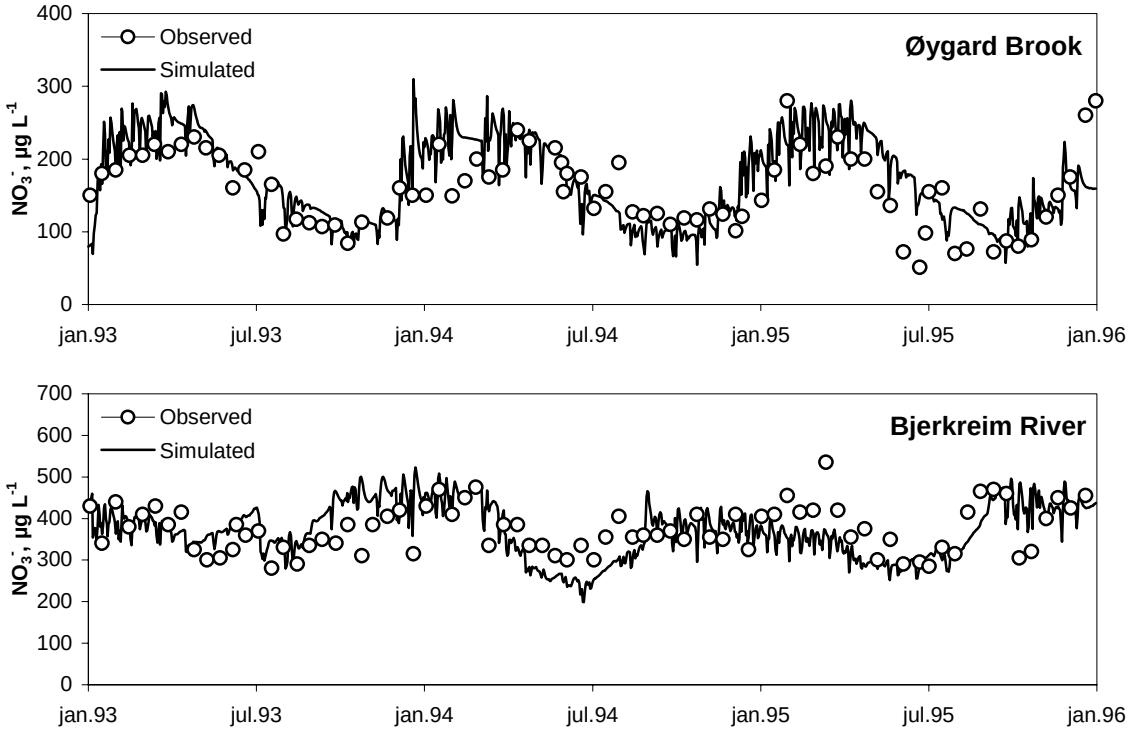

Figure 38. Simulated vs. observed NO_3^- concentrations at the Øygard catchment and at the Bjerkreim river outlet for the calibration period 1993-95.

Verification

To test the robustness of the 1993-95 calibration, the model was run for four additional years 1996-1999 at Øygard and the Bjerkreim river outlet. There are no observed data from Svela covering this period. The results from these verification runs were very close to those obtained from the model calibration (Table 10). However, the model did not capture the extremely high NO_3^- concentrations that appeared at Øygard during the exceptional cold winter in 1995/96 (Kaste and Skjelkvåle 2002), and the resultant r^2 value for the whole period was as low as 0.19. If excluding this period (15 Jan - 10 Apr 1996) from the dataset, the r^2 value increased to 0.47.

Table 10. INCA-N: Verification of the calibration based observed data for the period 1996-1999.

	Streamwater discharge		NO_3^- concentration	
	Mean (sim./obs. ratio)	Temporal pattern (r^2)	Mean (sim./obs. ratio)	Temporal pattern (r^2)
Bjerkreim river basin	0.99	0.74	0.93	0.18
Øygard catchment	0.99	0.82	1.12	0.19 / 0.47[a]

[a] extreme NO_3^- concentrations during the 1996 winter excluded

Control period (1980-1999)

Three hydrological datasets were generated by HBV for the control period 1980-99. These were based on (a) observed meteorological data, (b) the ECHAM4/OPYC3 AOGCM from the Max-Planck Institute, and (c) the HadAm3 AOGCM from the Hadley Centre. Although the datasets are generated by different sources, they largely describe the same climatological and hydrological patterns for the period 1980-99 (Figure 23 and Figure 24). When including the three hydrological datasets in INCA-N, the model results in terms of simulated NO_3^- concentrations show some small deviations on a monthly basis (Figure 39). However, relative to the annual variations and the uncertainties associated with the model simulations, the variations between the different control period datasets are negligible. Hence, the HBV runs based on observed climate were used as baseline for both the MPI 2030-49 and HAD 2080-99 scenarios.

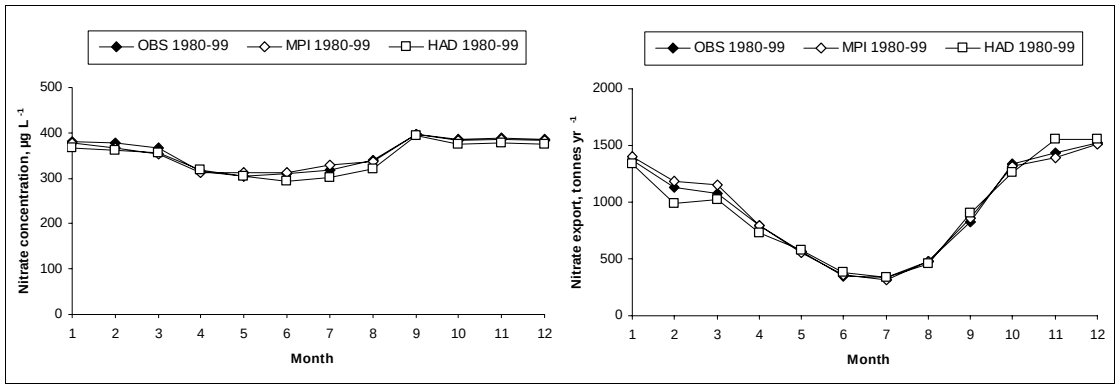

Figure 39. INCA-N simulated monthly mean NO_3 concentrations and fluxes at the Bjerkreim river outlet 1980-99, based on three hydrological datasets generated by the HBV model.

Future scenarios

The future scenarios for N cycling in the Bjerkreim basin include the 20-year periods 2030-49 (MPI) and 2980-99 (HAD). Whereas the MPI scenario indicates a moderate increase in both air temperature and precipitation amounts, the HAD scenario implies a much more dramatic increase in air temperatures and dryer summers and autumns. Both scenarios assume that N deposition is reduced according to current legislation (CLE). This is illustrated in Table 11, which shows the INCA-N simulated changes in N sources and sinks in the Bjerkreim basin given the two climate scenarios. Atmospheric deposition is the dominant N source in the basin, and the reduction in N inputs indicated in Table 11 is due to reduction in deposition alone. Fertiliser application and effluent discharges were assumed to remain constant over the modelling period. The lower N input in 2080-99 compared to 2030-49 is due to less precipitation in the Hadley scenario (Figure 18).

Table 11. Simulated terrestrial N balance in the Bjerkreim basin (kg N ha^{-1} yr^{-1}) given the MPI and Hadley (HAD) climate scenarios. Both scenarios include a reduction of N deposition corresponding to current legislation scenario (CLE).

	Control 1980-99	MPI 2030-49	HAD 2080-99
N sources			
NO_3^- input	13.6	10.3	9.8
NH_4^+ input	12.7	12.4	11.7
Net mineralisation	21.2	24.5	29.4
N fixation	0.0	0.0	0.0
Total	47.5	47.3	50.9
N sinks			
Plant uptake	8.9	10.0	11.4
Denitrification	4.9	4.6	5.9
Immobilisation	26.3	24.9	22.7
NO_3^- export	7.2	7.3	10.2
NH_4^+ export	0.4	0.7	0.8
Total	47.6	47.5	51.0
Balance	-0.2	-0.2	-0.1

In the MPI scenario, the reduced N deposition is to a great extent compensated by a temperature-driven increase in N mineralisation (16%) such that the total available N in the system is nearly

constant. Among the retention processes, two opposing factors are operating at the same time. First, the long-term accumulation of N in the system leads to decreased C:N ratio in the organic soil layer, which increases the risk of N leaching (Figure 6). Second, the increased temperature promotes vegetation growth and hence uptake of N. With the MPI scenario, INCA-N simulates a slight increase in the leaching of NO_3^- and NH_4^+ from the terrestrial parts of the basin. When including the Hadley scenario, N mineralisation increases by nearly 40% compared to the control period. This is partly compensated by reduced N deposition and increased uptake by vegetation, but counteracted by a reduction in the basin's ability to retain N. The result is increased leaching of NO_3^- and to a lesser extent NH_4^+ from the terrestrial parts of the basin.

At the Bjerkreim river outlet the INCA-N model simulates a 4% decrease in mean NO_3^- concentration but 4% increase in the mean flux with the MPI scenario for 2030-49 (Table 12). This indicates that increased temperature speeds up aquatic N retention processes and thus reduce NO_3^- concentrations. On the other hand, increased precipitation and streamwater flow increase the total NO_3^- export from the basin. With the Hadley scenario the streamwater NO_3^- concentrations and fluxes are predicted to increase by roughly 50% and 40%, respectively. Here, the predicted decrease in annual flow will reduce the NO_3^- export potential relative to the MPI scenario. NH_4^+ concentrations in the Bjerkreim river are low, usually below 25 µg N L^{-1} (based on 43 observation during 2000-2004). Both the MPI and the HAD scenario predict an increase in mean NH_4^+ concentrations (about 20 and 40%, respectively), but the changes in terms of absolute concentrations are low.

Table 12. Mean concentrations and fluxes of NO_3^- and NH_4^+ at the Bjerkreim river outlet in 1980-99, 2030-49, and 2081-2100. Standard deviations of annual values are indicated.

	NO_3^-		NH_4^+	
	µg N L^{-1}	tonnes N yr^{-1}	µg NL^{-1}	tonnes N yr^{-1}
1980-99 (observed)	356±42	561±59	17±2	26±4
2030-49 (MPI)	341±41	583±61	20±1	37±7
2080-99 (Hadley)	543±96	798±122	24±1	40±9

The climate change scenarios, especially for precipitation, have different seasonal patterns (see previous sections). Thus, the hydrological and hydrochemical signals from a future climate change will vary throughout the year. The MPI scenario produces lower NO_3^- concentrations during large parts of the year, except for the autumn and early winter when plant demand for N is low and streamwater flow is high (Figure 40). The seasonal NO_3^- signal simulated with the Hadley scenario is much stronger. NO_3^- concentrations are predicted to increase in all seasons, but especially during summer and autumn. In October, the simulated mean NO_3^- concentration exceeds the current levels by a factor of two. The reason for this dramatic NO_3^- leaching scenario seems to be the combination of increased temperature (which governs N mineralisation) and low-flow conditions with little dilution capacity. Thereafter increased precipitation from October and onwards seems to flush mineralised N out of the soil compartment.

Seasonal variations in solute chemistry may have a large influence on aquatic biota. In some cases, episodic events can be even more important - or critical when it comes to e.g. acidic pulses. The frequency of high NO_3^- concentrations will be much higher with the Hadley scenario compared to the MPI scenario and present (Figure 41). Here, NO_3^- concentration will exceed 800 µg N L^{-1} during 10% of the time and 1045 µg N L^{-1} during 1% of the time (73 days). The maximum NO_3^- concentration simulated with the Hadley scenario was 1340 µg N L^{-1}. Under these conditions, NO_3^- can be a significant contributor to surface water acidification when accompanied by hydrogen and aluminium ions from acidified parts of the basin. The frequency of low NO_3^- concentrations was about the same in the three 20-year periods.

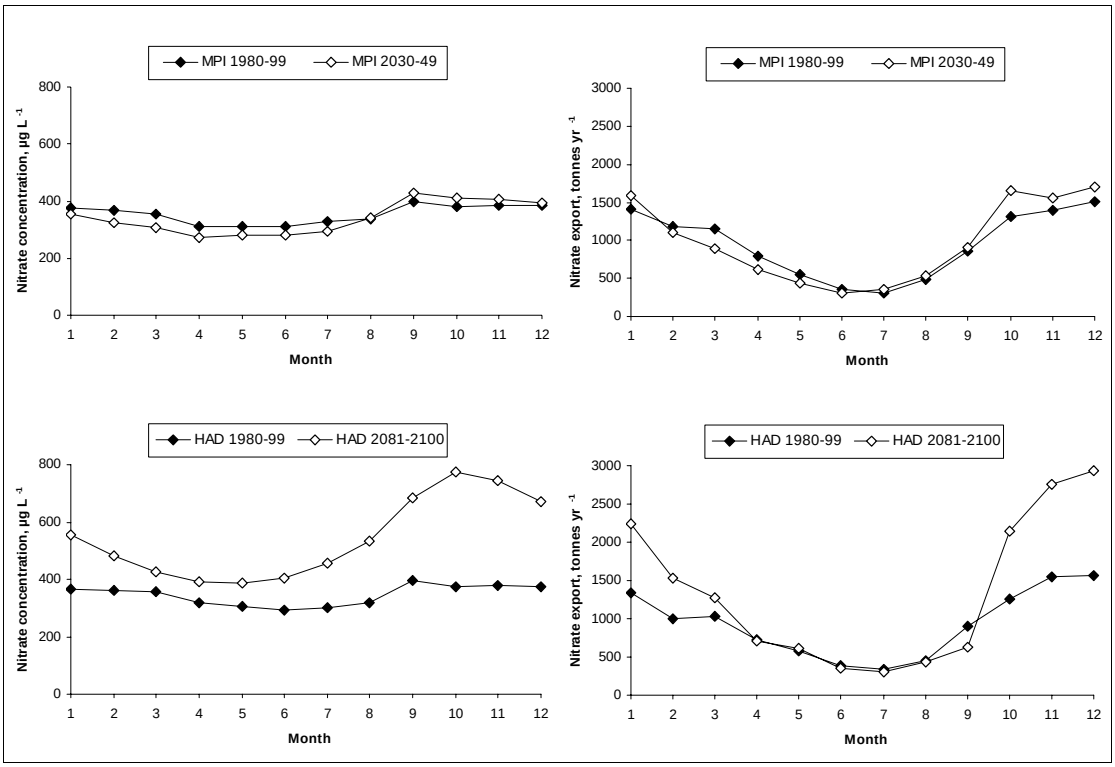

Figure 40. Monthly mean NO_3 concentrations and fluxes at the Bjerkreim river outlet in 2030-49 and 2081-2100, based on the MPI and HAD scenarios, respectively.

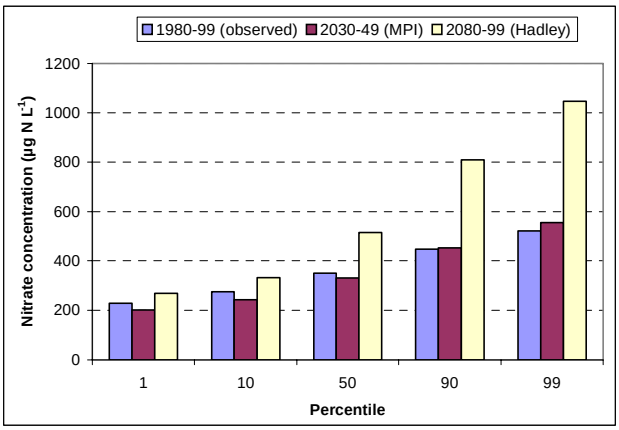

Figure 41. Frequency distributions of streamwater NO_3 concentrations (µg N L^{-1}) at the Bjerkreim river outlet, in 1980-99 (observed climate), 2030-49 (MPI) and 2080-99 (HAD).

3.4 Estuarine mixing and water quality (NIVA Fjord model)

In each scenario the NIVA Fjord model simulates a continuous time series through 20 years. In the present study, the relevant model variables were recorded each 10 days, and these recorded time series were used to make scenario comparisons. The first year was ignored, since it reflects common initial conditions. The results were aggregated to monthly means of the 4 upper layers (depth 0-2 m) of basin 3 and 4. Monthly averages were calculated for nitrate, phosphorus, silicate, and concentrations of silicon-dependent diatom and other phytoplankton (flagellates).

All the three runs for the control period showed about the same results for average conditions through the year, even though the specific time series were quite different. Figure 42 shows the resulting monthly average concentrations of nitrate and total particulate organic carbon, as a sum of

phytoplankton, zooplankton, bacteria and detritus from the biological processes in the estuary. The model includes only the organic matter that is produced within the estuarine model area, and not the organic matter in the river runoff, so it is expected that winter concentrations of organic carbon were simulated lower than what would actually be observed.

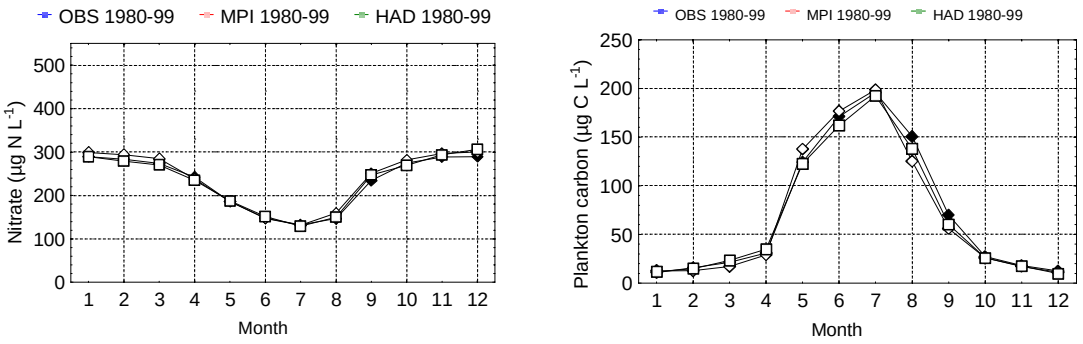

Figure 42. Monthly means of nitrate and particulate carbon in the Egersund estuary (middle basin) in the control period 1980-99, simulated by the NIVA fjord model on the basis of observed data and the MPI and Hadley scenarios.

The two future scenarios, MPI 2030-49 and HAD 2080-99 were run with identical outer boundary conditions and meteorological data as direct driving forces. The results are shown in Figure 43 with monthly average concentrations of nitrate and organic particulate carbon in the upper 2 m of basin 3. The results illustrate only the possible effect of climate induced changes in the runoff patterns (flow and concentrations of NO_3). They do not include corresponding changes in the coastal current, which could mean that effects are underestimated, if the same type of change occurred for other rivers, upstream in the coastal current. Nor do they include direct effects of climate changes, for instance changes in wind or cloudiness, which might affect vertical mixing and light limitation of primary production.

The upper part of Figure 43 shows the results of the MPI 2030-89 scenario, compared with the MPI control period. Nitrate was slightly reduced in spring, and somewhat increased in late autumn, and the effect on plankton was small. The HAD 2080-99 scenario in the lower part of the figure shows larger changes from the corresponding control scenario. The increased winter runoff of nitrate in Bjerkreim river was reflected in the estuary by a 50-100 % increase in average nitrate concentrations. In summer there was only a slight increase in residual nitrate concentrations in the surface layer of basin 3, but the model predicted a noticeable increase in particulate carbon of about 15-20 %. There were no major shifts in the composition; all plankton groups increased about equally. The model predicted an increase of about 5-10 % of the downward flux of dead organic matter through 4 m depth in the late summer months.

In basins 4 and 5 further out towards the open coastal water, the conditions were less influenced by the river runoff, and the predicted changes were generally smaller. A model run was done with the HAD 2080-99 scenario in combination with a general increase of air and runoff temperature by 3°C. This imposed temperature increase had almost no effect at all on the model results.

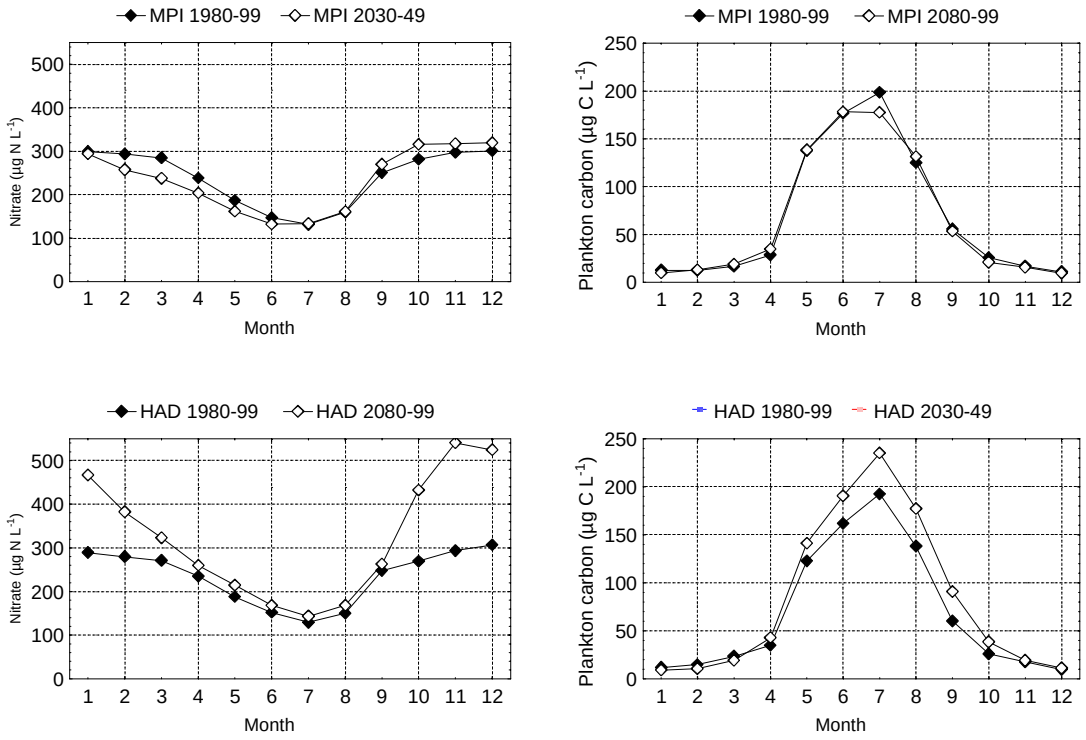

Figure 43. Monthly means of nitrate and particulate carbon in the Egersund estuary (middle basin) in the control period 1980-99, simulated by the NIVA fjord model on the basis of the MPI and Hadley scenarios for 2039-49 and 2080-99, respectively.

4. Discussion

4.1 Climate modelling and downscaling methods

The modelling of future climate involves a number of uncertainties as the understanding of the entire climate system with all relevant processes is incomplete. Furthermore, climate models cannot possibly explicitly account for every process at the very smallest scales. Hence, AOGCMs must be approximate descriptions of a large number of processes that take place on a spatial scale unresolved by the model grid boxes. For instance, the description of cloud processes, ocean currents, and vapour/energy exchange between the atmosphere and the surface vary with location and can only be described by a general approximation. A variety of climate models exist, and each model can give a different picture of the climate evolution (Cubasch *et al.* 2001). An example is given by (Benestad 2002) for 16 different model projections of temperature, empirically downscaled to different sites in Norway for the period 2000-2050 (Figure 44).

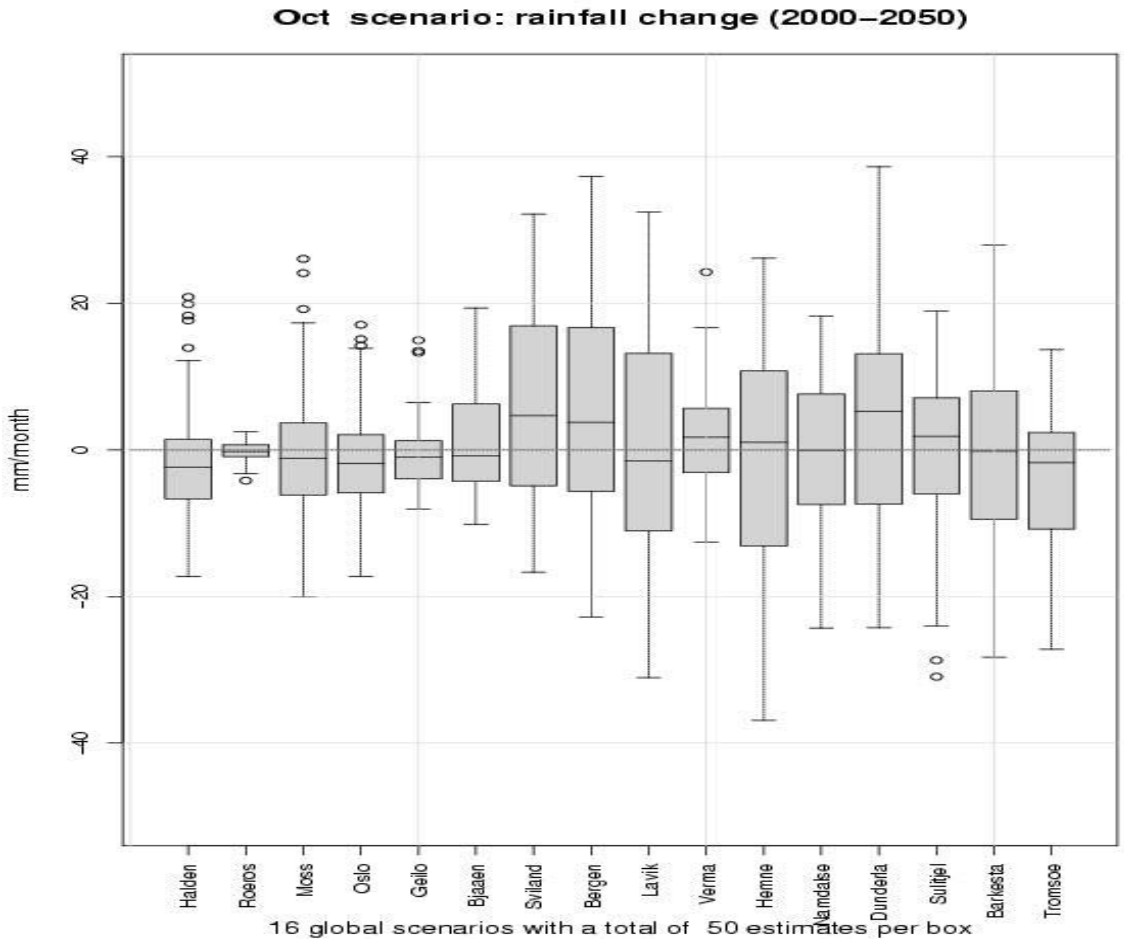

Figure 44. Projected mean monthly precipitation trend for October based on 16 different global scenarios for the period 2000-2050. The box shows the interquantile range (20-75 percentiles), the horizontal line gives the median value and the whiskers extend to the most extreme data points which are no more than 1.5 times the interquartile range from the box. From Benestad (2002).

Even if a climate model was perfect, there will be uncertainties associated with climate projections. Benestad (2000) noted that the climate model spin-up process is important for the description of the local climatic evolution, and that there were regional differences between four simulations done with

another Hadley model (HadCm2) for different initial conditions. These differences were regarded as a result of the non-linear chaotic behaviour of climate, and hence part of the unpredictable natural variability (Benestad 2001). It is also evident that these natural fluctuations affect the climate change analysis such as for 30-year long time slices. Benestad (2002) argued that part of the natural variations are 'externally forced' by, for instance, volcanoes, solar activity or landscape changes, and will therefore not be captured by climate models only driven with emission data.

Extreme events and projections of extreme events during the 21st century are of great importance for different research areas. IPCC summarises estimates of confidence in observed (Folland *et al.* 2001) and projected (Cubasch *et al.* 2001; Giorgi *et al.* 2001) changes in extreme weather and climate events. They found it likely that there is confidence in observed changes towards higher maximum temperatures and increased frequency of hot days, and also that confidence in the projected changes for the 21st century are very likely. The same is found for many other phenomena such as more intense precipitation events.

4.2 Evaluation of the multi-model approach

Simulation by modelling is a useful method for understanding and simulating the possible effects of climate change on ecosystems. Individual models, however, may be most detailed within their specific scientific field, and only make generalizations about other related parts of the ecosystem. Differences in scale and time resolution may be a problem when linking models. For the effect models HBV, INCA-N, MAGIC and the NIVA Fjord model there seems to be no major discrepancies with regard to scale. The HBV model has been set up for all the small catchments and sub-basins run by the INCA-N and MAGIC models. Further the simulated runoff for the sub-basins was accumulated to give total runoff of water and NO_3 for the Bjerkreim river basin as input to the NIVA Fjord Model. The HBV results for the Svela catchment may indicate the difficulties of capturing the dynamics in very small catchment (0.5 km^2). With regard to time resolution daily values from the HBV model have been applied directly to INCA-N and the Fjord model, whereas aggregated to yearly values for the MAGIC model.

The use of the output of one model as the input to the next requires that the different models operate on the same ecosystem description to ensure producing scientifically sensible results. The HBV model produces estimates of runoff to all the other models in the study. In addition the model produces area precipitation and average-height-adjusted T to the MAGIC model and estimates of HER and SMD to the INCA-N model. The INCA-N model has a detailed description of N processes, but only simple equations for HER and SMD. Hence, the model performed better with input data from HBV, which is a pure and conceptual hydrological model with the soil moisture zone as a central part (Sælthun 1996). With temperature and moisture dependent rate coefficients of N processes and daily time steps, the INCA model is more suitable than the MAGIC model to produce time series of inorganic N for the Fjord model. However, the INCA-N model lacks a dynamic soil organic pool, and thus MAGIC was used to simulate the long-term balance between N accumulation and release processes by applying soil carbon to nitrogen dynamics. On this basis, N immobilisation rates within INCA-N could be adjusted to match time series of N retention and losses generated by the MAGIC model. An annual time step was regarded sufficient in this particular MAGIC – INCA interaction.

The approach used in this study does not address possible feedback loops as the models are linked rather than coupled. In particular, the HBV model parametrisation is kept unchanged throughout the simulation periods. In practice, this presupposes that vegetation changes during the scenario period are not large enough to generate significant hydrological effects through changes in snow drift, vegetation interception or the relationship between climatic variables and potential evapotranspiration.

4.3 Magnification effects

Even small changes in the future climate may have effects on a river basin scale that may magnify when projected through the effect-chain from the climate system via hydrology, to water chemistry and biology. Most of these effects are inter-related and can not be assigned to one single climate parameter. Even though air temperature has a direct impact on snow accumulation and snowmelt, evapotranspiration and N transformation rates in soil and water, these processes are also affected by precipitation, wind, humidity, and several site-specific factors. Such complex interactions between factors along the climate change effect-chain make future projections difficult. Hence, there might be several chemical and biological outcomes from one single climate scenario, depending on other abiotic or biotic factors operating in the catchment.

As demonstrated in Figure 29 and Figure 30 increased winter temperatures will result in a significant decrease in snow accumulation. Besides increased winter flow and reduced springmelt flood, a reduction or even absence of a permanent snow cover may increase soil frost and also the frequency of freezing-thawing events. Both experimental studies and monitoring data have demonstrated that NO_3 concentrations in surface waters increased dramatically following periods of severe soil frost (Mitchell *et al.* 1996; Monteith *et al.* 2000; Groffman *et al.* 2001; Kaste and Skjelkvåle 2002). Freezing-thawing events might promote very high, episodic rates of mineralisation, nitrification and denitrification, where the net effect on surface water N concentrations might vary with hydrological load (Van Miegroet *et al.* 2001).

N transformation processes in catchments are temperature and moisture dependent, and a few degrees increase in air (and thereby soil) temperature may induce a significant increase in N process rates, depending on the Q_{10} value of the actual process (Figure 9). This is illustrated in this study by the increase in the N mineralisation rate in response to the MPI and HAD scenarios for temperature and precipitation in the Bjerkreim river basin (Table 11). Both laboratory experiments and large-scale experiments have suggested that decomposition and N mineralisation show a faster response to a temperature increase than the corresponding N retention processes, at least during an initial phase of the warming process (Kirschbaum 1995; Van Breemen *et al.* 1998). This may have important implications for N mineralisation and subsequent leaching of N to surface waters following climate change (Wright *et al.* 1998b).

Decades with elevated atmospheric N inputs have increased the soil internal N stores, and empirical data have demonstrated a negative correlation between NO_3 leaching rates and the C:N ratio of soil organic matter (Gundersen *et al.* 1998; Macdonald *et al.* 2002). Even after implementation of the Gothenburg protocol, the MAGIC model simulates a slight decrease in the C:N ratio of soil organic matter towards 2099. This implies a gradual increase in NO_3 leaching rates even with no climate change (Figure 35). With the MPI and the HAD climate scenarios, the decrease in C:N ratios and increase in NO_3 leaching rates will be more pronounced due to the combined effects of changed air temperature and precipitation amounts. This illustrates that climate change might accelerate the N saturation process and thus offset the effects expected from the Gothenburg protocol. To what extent this might happen, however, rely on several uncertain factors. Among these are: (i) the size of the N pool available for mineralisation, (ii) the amount of additional carbon sequestered due to climate change and thereby affecting the soil C:N ratio, and (iii) the actual temperature response (Q_{10} values) of the various N sink and source processes.

Whereas temperature to a large extent controls N production, hydrology is a key factor regulating the export of available N out of the catchments (Van Miegroet *et al.* 2001). Both the MPI and the HAD scenarios project an increase in streamwater flow during winter, when plant demand for N is close to zero and N is readily available in catchment soils. This results in higher streamwater N fluxes during winter (Table 12) that may cause acidification in poorly buffered surface waters and increased N loading on marine areas prior to the spring algal bloom. The warm and dry summers and early autumns projected by the HAD scenario will give more frequent and longer low-flow periods that may significantly reduce the recipient capacity of streams and lakes, and thereby promote increased

eutrophication problems. Additionally, S and N mineralised in soils during drought periods can generate large pulses of SO_4, NO_3, and NH_4 when soils are re-wetted (e.g., Dillon *et al.* 1997; Reynolds *et al.* 1992).

4.4 Specific effects related to the Bjerkreim river and the Egersund estuary

In the Bjerkreim river, the projected change in streamwater flow pattern and N dynamics may have important implications for water quality as well as freshwater biota. The river system is severely affected by acidification, and several species have been lost or damaged (Walseng *et al.* 2001). Since 1996, the main river has been limed to protect acid-sensitive organisms and especially the population of Atlantic salmon. In addition to relatively high S deposition, the Bjerkreim area is located in the part of Norway receiving the highest amounts of atmospheric N deposition (15-23 kg N ha^{-1} yr^{-1} during the 1990s). As a result, upland areas that are characterised by thin soils and sparse vegetation have experienced high leaching of inorganic N (Kaste *et al.* 1997). This excess N may promote acidification of surface waters, and during 1993-1995 inorganic N was estimated to account for up to 40% of the surface water acidity in the upper parts of the Bjerkreim river basin, on an annual basis (Henriksen *et al.* 1997).

Provided full implementation of the Gothenburg protocol of the UN-ECE Convention on Long-range Transboundary Air Pollutants and other legislation towards 2010, the S and N deposition in the Bjerkreim area are expected to decrease relative to 1990 levels by 70 and 35%, respectively (Schöpp *et al.* 2003). However, climate change might accelerate the N saturation process and thereby offset some of the water quality improvements expected after fulfilment of the Gothenburg protocol. Additionally, the projected change in streamwater flow patterns (floods, droughts) might affect the physical habitats for freshwater biota.

The lower parts of the river basin are affected by nutrient inputs from agriculture and domestic wastewater. Owing to the usually high streamwater flow, the dilution capacity is good and overall water chemistry is relatively little affected by the local pollution sources. However, the reduced flow during summer and early autumn projected by the HAD scenario implies a significant reduction of this recipient capacity, and dramatic increases in streamwater NO_3 concentrations (as well as other pollution agents) can be expected (Figure 39). This in combination with high water temperatures may govern growth of benthic algae and macrophytes that, in contrary to lake phytoplankton, are found to be stimulated by N addition in oligotrophic sytems (Lindstrøm and Johansen, 1995; Lindstrøm et al., 2000; Lindstrøm 2001).

In the Egersund estuary, the Fjord model indicates that summer production may increase by 15-20 % with the Hadley scenario. Since this scenario not implies any increase in NO_3 fluxes during summer (Figure 40), the production increase may be a result of longer residence time of the surface layer due to reduced freshwater inputs. It thus seems that the changes in runoff patterns may have greater effect on algae production than the changes in nutrient conditions per se. Since the Fjord model runs only include the local effects of climate change, the model results must be regarded as minimum estimates. The projected climate change is expected to have similar effects in other rivers along the coast, upstream in the coastal current. Hence, the conditions in the coastal current also will change and thereby add to the local effect in each estuary along the coast.

4.5 Potential of linked models as predictive tools in catchment management

In water science linking of models for different systems is still a relatively new practice, encouraged by recent laws and legislations, like the EU Water Framework Directive (WFD), that require/promotes integrated water resource management in catchments and estuaries (all parts of the “water system”). There will be a need in the future for systems that facilitates effect studies and guidance, and sets of linked models such as the example here provide tools by which the WFD can be implemented. The WFD demands that for each river basin and associated estuary in Europe, plans must be drawn up and

implemented such that water conditions meet the criterion of "good ecological status" by the year 2016. In cases such as the Bjerkreim river where runoff of nutrients such as N threatens the nutrient balance of the estuary downstream, and where nitrate-induced acidification poses a problem for salmon fisheries, measures must be taken to assure that the criterion of good ecological quality is met in the future. Future climate change could exacerbate the problem of excess nitrogen and mean that the measures must be more stringent. The relative effect of various scenarios of alternative measures within the river basin to reduce N inputs (for example, changes in forestry practices, agricultural practices, and treatment of domestic wastewater) can be evaluated by means of the linked model set presented here. Further the effectiveness of such measures relative to external drivers such as nitrogen deposition, climate change, and nutrient inputs from the coastal current can be evaluated.

5. References

Benestad, R. E. 2000. Future climate scenarios for Norway based on empirical downscaling and inferred directly from AOGCM results, DNMI Klima 23/00. Norwegian Meteorological Institute, Oslo, 127 pp.

Benestad, R. E. 2001. The cause of warming over Norway in the ECHAM4/OPYC3 GHG integration. Int. J. Clim. 21: 371-387.

Benestad, R. E. 2002. Empirically downscaled multi-model ensemble temperature and precipitation scenarios for Norway. Journal of Climate 15: 3008-3027.

Bergström, S. 1976. Development and application of a conceptual runoff model for Scandinavian catchments, Department of Water Resources Engineering, Lund Institute of Technology, University of Lund, Sweden, pp.

Bjerkeng, B. 1994. Eutrophication model for the inner Oslo fjord. Report 2: Description of the contents of the model [in Norwegian]. Norwegian Institute for Water Research, Oslo, Report no. 3113, 134 pp.

Bjørge, D., Haugen, J. E., and Nordeng, T. E. 2000. Future climate in Norway, Research Report No. 103. Norwegian Meteorological Institute, Oslo, pp.

Bull, K. R., Achermann, B., Bashkin, V., Chrast, R., Fenech, G., Forsius, M., Gregor, H.-D., Guardans, R., Haussmann, T., Hayes, F., Hettelingh, J.-P., Johannessen, T., Krzyzanowski, M., Kucera, V., Kvæven, B., Lorenz, M., Lundin, L., Mills, G., Posch, M., Skjelkvåle, B. L., and Ulstein, M. J. 2001. Coordinated effects monitoring and modelling for developing and supporting international air pollution control agreements. WASP 130: 119-130.

Cosby, B. J., Ferrier, R. C., Jenkins, A., and Wright, R. F. 2001. Modelling the effects of acid deposition: refinements, adjustments and inclusion of nitrogen dynamics in the MAGIC model. Hydrology and Earth System Sciences 5: 499-518.

Cosby, B. J., Hornberger, G. M., Galloway, J. N., and Wright, R. F. 1985a. Modelling the effects of acid deposition: assessment of a lumped parameter model of soil water and streamwater chemistry. Water Resources Research 21: 51-63.

Cosby, B. J., Wright, R. F., Hornberger, G. M., and Galloway, J. N. 1985b. Modelling the effects of acid deposition: estimation of long term water quality responses in a small forested catchment. Water Resources Research 21: 1591-1601.

Cubasch, U., Meehl, G. A., Boer, G. J., and Stouffer, R. J. 2001. Projections of future climate change, p. 525-582. In Houghton, J. T., Ding, Y., Griggs, D. J., Noguer, M., van der Linden, P. J., Dai, X., Maskell, K. and Johnson, C. A. [eds.], Climate Change 2001: the Scientific Basis. Cambridge University Press.

Dillon, P. J., and Molot, L. A. 1990. The role of ammonium and nitrate in the acidification of lakes and forested catchments. Biogeochem. 11: 23-43.

Dillon, P. J., Molot, L. A., and Futter, M. 1997. The effect of El Nino-related drought on the recovery of acidified lakes. Env.Monit.Assess. 46: 105-111.

Engen-Skaugen, T. 2004. Refinement of dynamically downscaled precipitation and temperature scenarios, Report No 15/04. Norwegian Meteorological Institute, Oslo, pp.

Folland, C. K., Karl, T. R., Christy, J. R., R.A., C., Gruza, G. V., Jouzel, J., Mann, M. E., Oerlemans, J., Salinger, M. J., and Wang., S.-W. 2001. Observed climate variability and change, p. 99-181. In Houghton, J. T., Ding, Y., Griggs, D. J., Noguer, M., van der Linden, P. J., Dai, X., Maskell, K. and Johnson, C. A. [eds.], Climate Change 2001: the Scientific Basis. Cambridge University Press.

Freeman, C., Evans, C. D., Monteith, D., and Fenner, N. 2001. Export of organic carbon from peat soils. Nature: 785-785.

Frei, C., Christensen, J. H., Déqué, M., Jacob, D., Jones, R. G., and Vidale, P. L. 2003. Daily Precipitation Statistics in Regional Climate Models: Evaluation and Intercomparison for the European Alps 10.1029/2002JD002287. Journal of Geophysical Research 108: Art. No. 4124.

Førland, E. J., Roald, L., Tveito, O. E., and Hanssen-Bauer, I. 2000. Past and future variations in climate and runoff in Norway, Report 19/00 Klima. Norwegian Meteorological Institute, Oslo, pp.

Giorgi, F., Hewitson, B., Christensen, J., Hulme, M., Von Storch, H., Whetton, P., Jones, R., Mearns, L., and Fu, C. 2001. Regional climate information -- evaluation and projections, p. 583-638. In Houghton, J. T., Ding, Y., Griggs, D. J., Noguer, M., van der Linden, P. J., Dai, X., Maskell, K. and Johnson, C. A. [eds.], Climate Change 2001: the Scientific Basis. Cambridge University Press.

Gordon, C., Cooper, C., Senior, C. A., Banks, H., Gregory, J. M., Johns, T. C., Mitchell, J. F. B., and Wood, R. A. 2000. The simulation of SST, sea ice extents and ocean heat transports in a version of the Hadley Centre coupled model without flux adjustments. Climate Dynamics 16: 147-168.

Groffman, P. M., Driscoll, C. T., Fahey, T. J., Hardy, J. P., Fitzhugh, R. D., and Tierney, G. L. 2001. Colder soils in a warmer world: a snow manipulation study in a northern hardwood forest ecosystem. Biogeochem. 56: 135-150.

Gundersen, P., Callesen, I., and de Vries, W. 1998. Nitrate leaching in forest ecosystems is controlled by forest floor C/N ratio. Environmental Pollution 102: 403-407.

Haugen, J. E., and Ødegaard, V. 2003. Evaluation of MPI and Hadley simulations with HIRHAM and sensitivity to integration domains, RegClim Phase III-General Technical Report No. 7. 19-29 pp.

Henriksen, A., and Hessen, D. O. 1997. Whole catchment studies on nitrogen cycling: Nitrogen from mountains to fjords. Ambio 26: 254-257.

Henriksen, A., Hindar, A., Hessen, D. O., and Kaste, Ø. 1997. Contribution of nitrogen to acidity in the Bjerkreim River in southwestern Norway. Ambio 26: 304-311.

Kaste, Ø. 2004. Simulation of nitrogen dynamics and losses in an arctic brook and a boreal river system in Norway by applying the Integrated Nitrogen model for CAtchments (INCA). Water Air and Soil Pollution Focus 4: 86-96.

Kaste, Ø., and Dillon, P. J. 2003. Inorganic nitrogen retention in acid-sensitive lakes in southern Norway and southern Ontario, Canada – a comparison of mass balance data with an empirical N retention model. Hydrological Processes 17: 2393-2407.

Kaste, Ø., and Skjelkvåle, B. L. 2002. Nitrogen dynamics in runoff from two small heathland catchments representing opposite extremes with respect to climate and N deposition in Norway. Hydrology and Earth System Sciences 6: 351-362.

Kaste, Ø., Henriksen, A., and Hindar, A. 1997. Retention of atmospherically-derived nitrogen in subcatchments of the Bjerkreim River in southwestern Norway. Ambio 26: 296-303.

Killingtveit, Å, and Sælthun, N.R. 1995. Hydrology. Vol 7 in Hydropower Development, Norwegian Institute of Technology (NTNU), 213 pp

Kirschbaum, M. U. F. 1995. The temperature dependence of soil organic matter decomposition, and the effect of global warming on soil organic C storage. Soil Biology and Biochemistry 27: 753-760.

Lindstrøm, E.-A. 2001. Increased vegetation growth in remote mountain lakes: An interaction between long-range transported air pollution and climate? [English summary] Norwegian Institute for Water Research, Oslo, Report no. 4459, 41 pp.

Lindstrøm, E.-A. and Johansen, S.W. 1995. Factors controlling periphyton growth in three rivers of low nutrient content. Experiments with nutrient-diffusing substrates in 1994. In: 'Nitrogen from mountains to fjords', Newsletter nr.3, Norwegian Institute for Water Research, Oslo, pp. 15-17.

Lindstrøm, E.-A., Kjellberg, G. and Wright, R.F. 2000. Critical loads for nutrient-nitrogen in Norwegian mountain lakes: Increased periphyton growth? [English summary] Norwegian Institute for Water Research, Oslo, Report no. 4187, 39 pp.

MacDonald, J. A., Dise, N. B., Matzner, E., Armbruster, M., Gundersen, P., and Forsius, M. 2002. Nitrogen input together with ecosystem nitrogen enrichment predict nitrate leaching from European forests. Global Change Biology 8: 1028-1033.

Mitchell, M. J., Driscoll, C. T., Kahl, J. S., Likens, G. E., Murdoch, P. S., and Pardo, L. H. 1996. Climatic control of nitrate loss from forested watersheds in the northeast United States. Environmental Science and Technology 30: 2609-2612.

Monteith, D. T., Evans, C. D., and Reynolds, B. 2000. Are temporal variations in the nitrate content of UK upland freshwaters linked to the North Atlantic Oscillation? Hydrological Processes 14: 1745-1749.

Moy, F.E. (Ed.), 2004. Long-term monitoring of environmental quality in the coastal regions of Norway [English summary]. Norwegian Pollution Control Authority (SFT), Oslo, Report no. 901/04, 79 pp.

Mulder, J., Nilsen, P., Stuanes, A. O., and Huse, M. 1997. Nitrogen pools and transformations in Norwegian forest ecosystems with different atmospheric inputs. Ambio 26: 273-281.

Palmer, T. N., and Räisänen, J. 2002. Quantifying the risk of extreme seasonal precipitation events in a changing climate. Nature 415: 512-514.

Rankinen, K., Kaste, Ø., and Butterfield, D. 2004. Adaption of the Integrated Nitrogen Model for Catchments (INCA) to seasonally snow-covered catchments. Hydrology and Earth System Sciences 8: 695-705.

Reynolds, B., Emmett, B.A., and Woods, C. 1992. Variations in streamwater nitrate concentrations and nitrogen budgets over 10 years in a headwater catchment in mid-Wales. Journal of Hydrology 136: 155-175.

Roald, L.A., Beldring, S., Væringstad, T., Engeset, R., Engen-Skaugen, T. and Førland, E.J. 2002.

Scenarios of annual and seasonal runoff for Norway based on climate scenarios for 2030-49. Rapport Klima 19, Norwegian Meteorological Institute, Oslo, p 9

Roeckner, E., Bengtsson, L., Feichter, J., Lelieveld, J., and Rodhe, H. 1999. Transient climate change simulations with a coupled atmosphere-ocean GCM including the tropospheric sulphur cycle. Journal of Climate 12: 3004-3032.

Schöpp, W., Posch, M., Mylona, S., and Johansson, M. 2003. Long-term development of acid deposition (1880-2030) in sensitive freshwater regions in Europe. Hydrology and Earth System Sciences 7: 436-446.

SFT. 2004. Norwegian monitoring programme for long-range transported air pollutants. Annual report - Effects 2003, Report 913/2004. The Norwegian Pollution Control Authority (SFT), Oslo, Norway, 1-172 pp.

Shaw, E. M. 1994. Hydrology in Practice - 3rd ed. Chapman and Hall. London, UK, 569 p

Sjøeng, A. M. 1998. Nitrogenomsetning i et heifelt, Øygard i Bjerkreimsvassdraget. University of Oslo, Norway

Skjelkvåle, B. L., Mannio, J., Wilander, A., and Andersen, T. 2001. Recovery from acidification of lakes in Finland, Norway and Sweden 1990-1999. Hydrology and Earth System Sciences 5: 327-338.

Stoddard, J. L., Jeffries, D. S., Lükewille, A., Clair, T. A., Dillon, P. J., Driscoll, C. T., Forsius, M., Johannessen, M., Kahl, J. S., Kellogg, J. H., Kemp, A., Mannio, J., Monteith, D., Murdoch, P. S., Patrick, S., Rebsdorf, A., Skjelkvåle, B. L., Stainton, M. P., Traaen, T. S., van Dam, H., Webster, K. E., Wieting, J., and Wilander, A. 1999. Regional trends in aquatic recovery from acidification in North America and Europe 1980-95. Nature 401: 575-578.

Sælthun, N. R. 1996. The "Nordic" HBV Model. Description and documentation of the model version developed for the project Climate Change and Energy Production, NVE Publication 7. Norwegian Water Resources and Energy Administration ISBN 82-410-0273-4, Oslo, 26 pp.

Sælthun, N. R., Aittoniemi, P., Bergström, S., Einarsson, K., Jóhannesson, T., Lindström, G., Ohlsson, P.-E., Thomsen, T., Vehviläinen, B., and Aamodt, K. O. 1998. Climate change impacts on runoff and hydropower in the Nordic countries, TemaNord 1998:552. Nordic Council of Ministers, Copenhagen, 170 pp.

Tveito, O. E., Førland, E. J., Heino, R., Hanssen-Bauer, I., Alexandersson, H., Dahström, B., Drebs, A., Kern-Hansen, C., Jónsson, T., Vaarby Laursen, E., and Westman, Y. 2000. Nordic temperature maps, Klima Report no. 09/00. Norwegian Meteorological Institute, Oslo, pp.

Tørseth, K., and Semb, A. 1997. Atmospheric deposition of nitrogen, sulfur and chloride in two watersheds located in southern Norway. Ambio 26: 258-265.

Tørseth, K., and Semb, A. 1998. Deposition of nitrogen and other major inorganic compounds in Norway, 1992-1996. Environmental Pollution 102: 299-304.

UN/ECE. 2002. http://www.unece.org/env/lrtap/

van Breemen, N., Jenkins, A., Wright, R. F., Arp, W. J., Beerling, D. J., Berendse, F., Beier, C., Collins, R., van Dam, D., Rasmussen, L., Verburg, P. S. J., and Wills, M. A. 1998. Impacts of elevated carbon dioxide and temperature on a boreal forest ecosystem (CLIMEX project). Ecosystems 1: 345-351.

van Miegroet, H., Creed, I. F., Nicholas, N. S., Tarboton, D. G., Webster, K. L., Shubzda, J., Robinson, B., Smoot, J., Johnson, D. W., Lindberg, S. E., Lovett, G. M., Nodvin, S., and Moore, S. 2001. Is there synchronicity in nitrogen input and output fluxes at the Noland Divide watershed, a small N-saturated forested catchment in the Great Smoky Mountians National Park? In: Optimizing Nitrogen Management in Food and Energy Production and Environmental Protection: Proceedings of the 2nd International Conference on Science and Policy. TheScientificWorld 1(S2): 480-492.

Wade, A. J., Durand, P., Beaujouan, V., Wessel, W. W., Raat, K. J., Whitehead, P. G., Butterfield, D., Rankinen, K., and Lepisto, A. 2002. A nitrogen model for European catchments: INCA, new model structure and equations. Hydrology and Earth System Sciences 6: 559-582.

Walseng, B., Langåker, R., Brandrud, T.E., Brettum, P., Fjellheim, A., Hesthagen, T., Kaste, Ø., Larsen, B.M., and Lindstrøm, E.-A. 2001. The river Bjerkreim in SW Norway – successful chemical and biological recovery after liming. Water Air Soil Pollut. 130: 1331-1336.

Whitehead, P. G., Wilson, E. J., and Butterfield, D. 1998. A semi-distributed Integrated Nitrogen model for multiple source assessment in Catchments (INCA): Part I – model structure and process equations. Science of the Total Environment 210: 547-558.

Wright, R. F. 1998. Effect of increased CO2 and temperature on runoff chemistry at a forested catchment in southern Norway (CLIMEX project). Ecosystems 1: 216-225.

Wright, R. F., Beier, C., and Cosby, B. J. 1998b. Effects of nitrogen deposition and climate change on nitrogen runoff at Norwegian boreal forest catchments: The MERLIN model applied to Risdalsheia (RAIN and CLIMEX projects). Hydrology and Earth System Sciences 2: 399-414.

Wright, R. F., Emmett, B. A., and Jenkins, A. 1998a. Acid deposition, land-use change and global change: MAGIC7 model applied to Risdalsheia, Norway (RAIN and CLIMEX projects) and Aber, UK (NITREX project). Hydrology and Earth System Sciences 2: 385-397.

Aas, W., Solberg, S., Berg, T., Manø, S., and Yttri, K. E. 2004. Overvåking av langtransportert forurenset luft og nedbør. Atmosfærisk tilførsel 2003., 903/2004. Statens forurensningstilsyn, Oslo, Norge, 166 pp.

Appendix A. HBV parameters – small catchments

Hypsographic curves

Øygard		**Svela**		**Apeland**	
Elevation (masl)	% of catchment area below	Elevation (masl)	% of catchment area below	Elevation (masl)	% of catchment area below
180	0	160	0	50	0
200	1	200	3	60	13
300	7	240	12	80	19
320	14	260	18	100	24
340	22	300	27	116	35
360	33	320	35	132	43
400	43	340	42	160	53
420	55	360	46	180	67
460	67	400	67	200	86
500	90	440	91	220	90
542	100	498	100	258	100

Temperature gradient	**Øygard**	**Svela**	**Apeland**
TVGRAD -Temperature gradient for days with precipitation [C/100 m]	-0.45	-0.45	-0.45
PGRAD - Precipitation altitude gradient [1/100 m]	-0.03	-0.03	-0.03

Precipitation correction	**Øygard**	**Svela**	**Apeland**
PKORR - Precipitation correction for rain (1)	1.00	0.80	0.90
SKORR - Additional precipitation correction for snow at gauge (1)	1.20	1.20	1.20

Snow routine	**Øygard**	**Svela**	**Apeland**
TX – Threshold temperature for snow/ice [deg C]	- 0.50	- 0.50	- 0.50
TS – Threshold temperature for no melt [deg C]	- 0.50	- 0.63	- 0.50
CX – Melt index [mm/deg/day]	4.00	5.00	4.00

Soil moisture zone	**Øygard**	**Svela**	**Apeland**
FC - Maximum soil water content [mm]	150	150	150
FCDEL - Potential evapotranspiration when content = FC*FCDEL	0.70	0.70	0.70
BETA - Non-linearity in soil water zone	3.00	3.00	3.00
INFMAX - Maximum infiltration capacity [mm/day]	50.0	50.0	50.0

Dynamic module – Upper and lower zone	**Øygard**	**Svela**	**Apeland**
KUZ2 - Quick time constant upper zone [1/day]	0.50	2.00	0.80
UZ1 - Threshold quick runoff [mm]	30.0	15.0	30.0
KUZ1 - Slow time constant upper zone [1/day]	0.10	0.20	0.10
PERC - Percolation to lower zone [mm/day]	0.30	0.30	0.30
KLZ - Time constant lower zone [1/day]	0.01	0.01	0.01

Routing through lakes	**Øygard**	**Svela**	**Apeland**
ROUT1 - Routing constant (lake area, km2)	0.70	0.00	0.00
ROUT2 - Routing constant (rating curve const)	20.0	0.00	0.00
ROUT3 - Routing constant (rating curve zero)	0.00	0.00	0.00
ROUT4 - Routing constant (rating curve exp)	1.60	0.00	0.00
ROUT5 - Routing constant (drained area ratio)	0.75	0.00	0.00

Appendix B. HBV parameters – sub-basins

Hypsographic curves

Sub-basin 1

Elevation (masl)	% of catchment area below level
179	0
279	5
360	11
580	20
520	30
710	50
780	71
820	81
875	91
906	95
1080	100

Sub-basin 2

Elevation (masl)	% of catchment area below level
179	0
191	11
240	20
319	32
375	42
416	51
460	63
538	77
565	82
709	97
900	100

Sub-basin 3

Elevation (masl)	% of catchment area below level
167	0
220	8
340	19
480	30
560	40
615	51
680	71
746	87
818	95
880	99
937	100

Sub-basin 4

Elevation (masl)	% of catchment area below level
60	0
110	4
170	10
224	20
250	30
299	46
345	64
399	78
478	91
579	99
715	100

Sub-basin 5a

Elevation (masl)	% of catchment area below level
60	0
17	5
160	10
269	16
350	21
560	40
635	51
690	63
749	78
860	97
945	100

Sub-basin 5b

Elevation (masl)	% of catchment area below level
3	0
33	4
50	12
71	23
100	40
120	51
144	61
175	71
200	81
298	92
440	100

Sub-basin 6

Elevation (masl)	% of catchment area below level
3	0
25	7
40	12
73	23
91	36
117	48
120	65
139	69
151	80
180	96
220	100

Routing through lakes	**1**	**2**	**3**	**4**	**5a**	**5b**	**6**
ROUT1*	10.5	12	10.2	9.4	15.0	5.0	4.7
ROUT2 *	30.0	70.0	20.0	40.0	40.0	50.0	50.0
ROUT3 *	0.00	0.00	0.00	0.00	0.00	0.00	0.00
ROUT4 *	1.60	1.60	1.60	1.60	1.60	1.60	1.60
ROUT5*	1.00	1.00	1.00	1.00	1.00	0.75	1.00

*see details on parameter in table on previous page.

The other parameter values for the sub-basins are equal to the values for the Øygard catchment, except for the quick time constant upper zone KUZ2 which was set to 0.80 for all sub-basins.

Appendix C. INCA-N v. 1.9 parameters - Bjerkreim river basin 1993-95.

River Bjerkreim 1993-1995						
Land cover class (short name)	Forest	HeaMou	Peat	SVegF	Arable	Lake
Land cover class	Forest	Heath+montane	Peat	Pasture fert.	Arable	Lake surfaces
Surface flow (m3 s-1)	0.001	0.001	0.001	0.001	0.001	0.001
Sub-surface flow (m3 s-1)	0.001	0.001	0.001	0.001	0.001	0.001
Surface nitrate (mg N l-1)	0.4	0.4	0.4	0.4	0.4	0.4
Sub-surface nitrate (mg N l-1)	0.4	0.4	0.4	0.4	0.4	0.4
Surface ammonium (mg N l-1)	0.01	0.01	0.01	0.01	0.01	0.01
Sub-surface ammonium (mg N l-1)	0.05	0.05	0.05	0.05	0.05	0.05
Surface drainage volume (m3)	1000	10000	1000	1000	1000	10000
Sub-surface drainage volume (m3)	50000	50000	50000	50000	50000	100000
Start date	01/01/1993					
Number of days	1095					
Denitrification rate/day	0.01	0.003	0.1	0.02	0.02	4
Nitrogen fixation (kg N/ha/day)	0	0	0	0	0	0
Plant nitrate uptake rate/day	1	0.01	0.05	0.2	0.3	0
Maximum nitrate uptake (kg N/ha/year)	150	40	45	200	200	70
Nitrate addition rate (kg N/ha/day)	0	0	0	4	4	0
Nitrification rate/day	0.3	0.3	0.3	0.3	0.3	3
Mineralisation (kg N/ha/day)	0.3	0.2	0.2	1	1	0
Immobilisation rate/day	2	2	2	0.5	0.5	0
Ammonium addition rate (kg N/ha/day)	0	0	0	4	4	0
Plant ammonium uptake rate/day	1	0.01	0.01	0.1	0.1	0
Plant growth start day (julian day)	80	80	80	100	100	120
Plant growth period (days)	200	150	150	170	170	180
Fertiliser addition start day (julian day)	0	0	0	232	110	0
Fertiliser addition period (days)	0	0	0	15	20	0
Soil Moisture Deficit maximum (mm)	80	80	80	80	80	80
Maximum temperature difference (oC)	4.5	4.5	4.5	4.5	4.5	4.5
Denitrification temperature threshold (oC)	9999	9999	9999	9999	9999	9999
Nitrification temperature threshold (oC)	9999	9999	9999	9999	9999	9999
Mineralisation temperature threshold (oC)	9999	9999	9999	9999	9999	9999
Immobilisation temperature threshold (oC)	9999	9999	9999	9999	9999	9999
Minimum surface flow level (m3 s-1)	9999	9999	9999	9999	9999	9999
Minimum sub-surface flow level (m3 s-1)	9999	9999	9999	9999	9999	9999
Q10 - denitrification	1.5	1.5	1.5	1.5	1.5	1.5
Q10bas - denitrification	25	25	25	25	25	25
Q10 - N fixation	1.5	1.5	1.5	1.5	1.5	1.5
Q10bas - N fixation	25	25	25	25	25	25
Q10 - nitrification	5	5	5	5	5	5
Q10bas - nitrification	15	15	15	15	15	15
Q10 - mineralisation	4	4	4	4	4	4
Q10bas - mineralisation	15	15	15	15	15	15
Q10 - immobilisation	1.5	1.5	1.5	1.5	1.5	1.5
Q10bas - immobilisation	25	25	25	25	25	25
Q10 - nitrate uptake	1.5	1.5	1.5	1.5	1.5	1.5
Q10bas - nitrate uptake	25	25	25	25	25	25
Q10 - ammonium uptake	1.5	1.5	1.5	1.5	1.5	1.5
Q10bas - ammonium uptake	25	25	25	25	25	25
Initial snow depth (mm)	0	0	0	0	0	0
Degree-day factor for snowmelt (mm/oC/day)	3	3	3	3	3	3
Water equivalent factor	0.3	0.3	0.3	0.3	0.3	0.3
Snow depth factor	-0.025	-0.025	-0.025	-0.025	-0.025	-0.025
Thermal conductivity of soil	0.6	0.6	0.6	0.6	0.6	0.6
Specific heat capacity due to freeze/thaw	6.6	6.6	6.6	6.6	6.6	6.6
Soil reactive zone time constant (days)	1	2	1	1	1	10
Groundwater zone time constant (days)	20	50	20	20	20	50
VrMax (depth x porosity) (m)	1	0.4	1	1	1	10
Initial flow (m3/s)	10					
Initial NO3 concentraation (mg N/L)	0.4					
Initial NH4 concentration (mg N/L)	0.01					
Number of reaches	7					

Reach name	Length (m)	Flow a	Flow b	In-stream Denitr (/day)	In-stream Nitri. (/day)	Effluent NO3 (mg N/L)	Effluent NH4 (mg N/L)	Effluent Flow (m3/s)	Effluent input Yes=1
Maudal	30000	0.02	0.55	0.002	1.5	3.125	3.125	0.005	1
Byrkjeland	12000	0.02	0.55	0.002	1.5	3.125	3.125	0.01	1
Hofreiste	25000	0.05	0.7	0.002	1.5	3.125	3.125	0.01	1
Svela	25000	0.1	0.9	0.002	1.5	3.125	3.125	0.1	1
Orsdal	50000	0.05	0.7	0.002	1.5	3.125	3.125	0.01	1
Tengesdal	12000	0.1	0.9	0.002	1.5	3.125	3.125	0.04	1
Tengs	12000	0.1	0.9	0.002	1.5	3.125	3.125	0.01	1

Area (km2)	Forest%	HeaMou%	Peat%	SVegF%	Arable%	Lake%	Basefl. index	Atm. Dep. NO3d kg/ha/yr	Atm. Dep. NO3w kg/ha/yr	Atm. Dep. NH4d kg/ha/yr	Atm. Dep. NH4w kg/ha/yr
87	11	74	1	1	1	12	0.5	0.9	8.6	0.7	8.2
67	27	44	1	6	4	18	0.5	1	10	1.3	9.1
79	17	66	1	2	1	13	0.5	0.9	10.7	0.8	9.2
117	22	51	2	12	5	8	0.5	1.1	7.9	1.3	6.4
259	12	75	1	1	1	11	0.5	1.1	10	0.9	9.3
40	38	31	1	15	10	5	0.5	1.1	7.6	1.2	6
36	35	43	1	5	3	13	0.5	1.2	7.2	1.3	5.4